AD-A052 871 NAVAL ACADEMY ANNAPOLIS MD DIV OF ENGINEERING AND WEAPONS F/G 20/4
AN EXPERIMENTAL STUDY OF TURBULENT BOUNDARY LAYER WITH SLIT SUC--ETC(U)
MAR 78 S M CALISAL
UNCLASSIFIED USNA-EW-5-78 NL

| OF |

AD A052871

END
DATE
FILMED
5-78
DDC

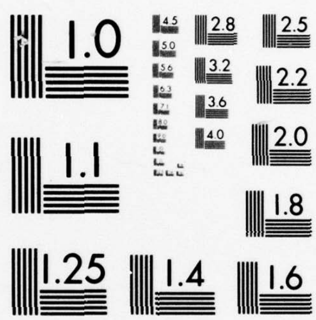

MICROCOPY RESOLUTION TEST CHART
NATIONAL BUREAU OF STANDARDS-1963-A

21

UNITED STATES NAVAL ACADEMY
DIVISION OF
ENGINEERING AND WEAPONS
ANNAPOLIS, MARYLAND

21

UNITED STATES NAVAL ACADEMY
Annapolis, Maryland 21402

DIVISION OF ENGINEERING AND WEAPONS

Report EW-5-78

An Experimental Study of Turbulent Boundary Layer with Slit Suction

Sander M. Calisal*

March 1978

*Assistant Professor
Naval Systems Engineering Department
U. S. Naval Academy
Annapolis, Maryland

This report was prepared in connection with a research grant from the U. S. Naval Academy Reserach Council (NARC)

SECURITY CLASSIFICATION OF THIS PAGE (When Data Entered)

REPORT DOCUMENTATION PAGE

READ INSTRUCTIONS BEFORE COMPLETING FORM

1. REPORT NUMBER: EW-5-78

(14) USNA-EW-5-78

2. GOVT ACCESSION NO.

3. RECIPIENT'S CATALOG NUMBER

4. TITLE (and Subtitle): (6) An Experimental Study of Turbulent Boundary Layer with Slit Suction.

5. TYPE OF REPORT & PERIOD COVERED: June 1976 - Dec 77 Final

6. PERFORMING ORG. REPORT NUMBER

7. AUTHOR(s): (10) Sander M./Calisal

8. CONTRACT OR GRANT NUMBER(s): (9) Final rept. Jun 76-Dec 77.

9. PERFORMING ORGANIZATION NAME AND ADDRESS: United States Naval Academy, Annapolis, Maryland 21402

10. PROGRAM ELEMENT, PROJECT, TASK AREA & WORK UNIT NUMBERS

11. CONTROLLING OFFICE NAME AND ADDRESS: United States Naval Academy, Annapolis, Maryland 21402

12. REPORT DATE: (11) March 1978

13. NUMBER OF PAGES: 42 (12) 48 p.

14. MONITORING AGENCY NAME & ADDRESS (if different from Controlling Office)

15. SECURITY CLASS. (of this report): Unclassified

15a. DECLASSIFICATION/DOWNGRADING SCHEDULE

16. DISTRIBUTION STATEMENT (of this Report)

Approved for public release; distribution unlimited.

17. DISTRIBUTION STATEMENT (of the abstract entered in Block 20, if different from Report)

18. SUPPLEMENTARY NOTES

19. KEY WORDS (Continue on reverse side if necessary and identify by block number)

Boundary layer, suction, slit, Turbulent

20. ABSTRACT (Continue on reverse side if necessary and identify by block number)

Experiments are performed on a flat plate with suction slit, in the Reynolds number range $5 \times 10^5 < Re < 1.1 \times 10^6$. Mean Velocity profiles, RMS values are measured with hot wire anemometry. Friction velocity is numerically calculated. The experiments showed that a classical boundary layer parameter α is related to the suction coefficient S_c with an equation of the form:

DD FORM 1473, 1 JAN 73 — EDITION OF 1 NOV 65 IS OBSOLETE — S/N 0102-014-6601

406 923

SECURITY CLASSIFICATION OF THIS PAGE (When Data Entered)

$$\ln\left(\frac{\alpha \text{ with suction}}{\alpha \text{ without suction}}\right) = A \cdot S_c + B$$

The value of A ssems to depend strongly on the relative location with respect to suction slit and possibly weakly on Reynolds number.

ABSTRACT

Experiments are performed on a flat plate with a transverse suction slit in the Reynolds number range $5 \times 10^5 < Re < 1.1 \times 10^6$. Mean Velocity profiles, RMS values are measured with hot wire anemometry. Friction velocity is numerically calculated. The experiments showed that a classical boundary layer parameter α is related to the suction coefficient S_c with an equation of the form:

$$\ln \left(\frac{\alpha \text{ with suction}}{\alpha \text{ without suction}} \right) = A \cdot S_c + B \qquad \text{for } 0 < S_c < 3 \text{ and } y^* > 10$$

The value of A seems to depend strongly on the relative location with respect to suction slit and possibly weakly on Reynolds number.

Table of Contents

Nomenclature

R_e	Reynolds number $R_e = \frac{U.L}{\nu}$
$S_c = \frac{S.P.}{U}$	suction coefficient
S.P.	Mean suction velocity at the slit
U	Mean stream velocity
u	local mean velocity in the boundary layer
u_τ	friction velocity $u_\tau = \sqrt{\tau w/\rho}$
y	Vertical distance measured from the wall
y*	$u_\tau\, y/\nu$
α	a classical boundary layer parameter
τ_w	wall shear stress
ν	Kinematic viscosity coefficient
RMS	Defined as RMS $= \sqrt{\frac{1}{T}\int^T U^2\, dt}$

INTRODUCTION

In the past suction or injection has been successfully used to prevent separation, to relaminarize flow, to obtain minimum viscous resistance or to decrease heat flux. Suction for such purposes has been used in VTOL aeroplanes, rocket nozzles, and also in the experimental resistance measurement of an "optimum" ship Calisal(1972). In this last case suction was applied to decrease the effect of separation at the stern of a ship model. It was found that for the model design Froude number a small amount of suction reduced the total resistance of the model to a value predicted by the optimization procedure, seemingly establishing the validity of a linearized potential solution and its application to optimization techniques.

An unsolved problem still existed, however, in the interpretation of the results and in model-ship correlation. In towing tank experiments turbulence is artificially generated by a wire or by a similar arrangement. The introduction of suction in the boundary layer of the model might "relaminarize" the flow around the model. Under these conditions the standard model-ship correlation will be incorrect as the model and the ship move at different Reynold's numbers. The amount of suction that seems to be effective at the Reynold's number of a model can possibly be ineffective at the Reynold's number of a ship. One can also claim that the effectiveness of suction is limited to models where relaminarization takes place, and this relaminarization is responsible for the decrease in the total resistance.

The purpose of this investigation was to establish the conditions necessary for relaminarization and its boundaries, and to determine whether such conditions existed in the previously mentioned experiment. This required a certain amount of turbulent boundary layer experimentation. The proposed problem was then studied as an inverse problem, that is, the study of the changes in the turbulent boundary layer characteristics due to slit suction. The rate of suction was kept as a variable, as the required suction rate for relaminarization was an unknown.

The effect of suction on laminar boundary layers has been thoroughly investigated both theoretically and experimentally. Due to complexities however similar studies are limited on turbulent boundary layers. Tennekes (1965) Bradshaw (1966, 1969), Black and Sarnecki (1965) studied turbulent boundary layers with suction or injection. Most of the existing theories are, unfortunately, for uniformly distributed suction and steady outer flows. It was therefore very difficult both to estimate the magnitude of suction requires for relaminarization and to calculate the variation in the boundary layer parameters due to slit suction. In addition to these problems there still remains the problem of identifying laminar, turbulent and transition flows. Such identifications are complicated by the deceptive nature of transient flows.

A second equally important parameter is the pressure gradient of the outer flow. This parameter and its influence on relaminarization was studied by Patel (1968). From experimental evidence he concluded that a strong, favorable pressure gradient can also relaminarize flow. Based on this study Bradshaw (1969) developed a theoretical "reverse transition criterion".

In this present investigation the effect of strong pressure gradients are excluded, even though they are of interest to naval architects. This parameter will be studied separately, as pressure gradients always exist around ship hulls

The purpose of this investigation can be summarized as a study to determine the effect of a suction slit on a turbulent boundary layer and to record the occurance of relaminarization and its limits.

EXPERIMENTS

Wind Tunnel

Experiments were made in the U. S. Naval Academy Pyle low speed, open circuit wind tunnel. This tunnel is equipped with honeycomb sections which permit a low level turbulence in the flow. The test section is one foot square, and the contraction ratio is sixteen to one. The maximum velocity in the tunnel is about 73 ft/sec. The velocity is controlled by a damper at the exit end. The expected ambient turbulence intensity in the test section is about 1%.

Model

A flat plate model was constructed with a suction slit one eighth of an inch in width and eleven inches in length. A one inch ID pipe was used to remove the boundary layer. A smooth curve completed the other face of the model. This curvature is used to decrease the effect of piping on the main flow. The flat surface was leveled to generate a minimum pressure gradient along the flow direction and eleven pressure taps were used to measure the static pressure. The location of pressure taps and related dimensions are given in figure 1.

DATA ACQUISITION SYSTEM

Figure 2 gives the calibration and instrumentation system used for velocity measurement. This consists mainly of a boundary-layer-type probe which sends the information to the DISA 55M01 Main unit through a standard bridge. No boosters are used. The signal is then sent to a DISA55M25 linearizer. The linearizers output is further used to find the RMS value of the signal. The linearizer output and the related RMS value are read by DISA 55D31 Digital voltmeters.

The Calibration of the hot wire probe is done with the DISA calibration equipment for the range 5-25 m/sec. The pressure drop in the calibration tunnel is measured with an electrical pressure transducer, which gives a digital output. The calibration of the system and the linearizer's settup are checked with an x-y plotter. The settings are adjusted to have a linear relationship between the theoretical velocity obtained from the pressure drop readings at the calibration tunnel and the velocity as indicated by the M55 system. A linear regression curve fit is then used to obtain calibration parameters. The initial calibration of the pressure transducer is made using a calibration manometer. The location of the probe wire with respect to the flat plate is measured optically and the expected accuracy of this measurement is 0.02mm.

The visually observed data for velocity and RMS are manually recorded in files in the U. S. Naval Academy main computer. Pressure readings on the other hand are automatically recorded with a scanivalve coupled to DAS-2 and a Tektronix 4051 computer. DAS-2 is a locally manufactured data acquisition system. These readings are recorded on a casette tape. Plots of the data are usually obtained with a hard copier connected to the Tektronix terminal. The data thus obtained are stored in the main computer for further processing.

An attempt was also made to study the frequency spectrum of the turbulence. Unfortunably this could not be continued because of the calibration problems encountered with the available tape recorder.

EXPERIMENTS

Nineteen separate experiments were performed each with a different uniform velocity and variable suction rate. The maximum values of suction and mean flow correspond to the maximum values obtainable by the existing equipment, and the lower limits are those corresponding to a stable flow. Since the mean velocity of the flow is regulated by a damper, certain unsteady flow characteristics were reported at low speeds. For each experiment the required checks and adjustments recommended by DISA were made, and the probes calibrated as described above (Ref. 10). For the selected speeds velocity profiles and RMS values were first obtained to calibrate the overall system. Three points one two inches downstream from the suction slit (Point A) Figure 1. Another 2" up-stream from the slit (Point B) and the third 4" down stream from the slit (Point C) were selected as the test points. In this selection the important consideration was to be as close as possible to the slit, but yet far enough away from it that the flow in the direction perpendicular to the plate is negligeable. Otherwise, one will be forced to measure that component simultaneously. The minimum distance to the wall was about 0.2 mm. The probe traverse mechanism made possible the change of this distance by 0.01 mm, but 0.1 mm increments are used during these experiments.

The suction rate was changed up to the maximum suction coefficient $S_C = 2.5$ for various experiments. The Reynolds number range based on the distance from the leading edge to the slit is $3 \times 10^5 < Re < 1.1 \times 10^6$

RESULTS OF EXPERIMENTS

MEASURED QUANTITIES

During these experiments velocity profiles and corresponding RMS values were measured and recorded. Some typical observations can be summarized as follows. For point A two inches downstream from the slit the velocity profile showed an augmentation of velocity up to a point comparable to the boundary layer thickness, and a decrease of velocity beyond that point (Figure 3). The net effect on velocity seems to suggest a virtual vortex located at about the boundary layer thickness. The change in profiles do not show a linear dependence on suction quantity. Rather a relatively small suction quantity seem to accelerate the flow with a higher "efficiency". RMS values measured at point A showed a drastic change in their distribution. One can possibly explain this as being the result of the shift of the outer laminar flow closer to the wall (Figure 4). The maximum RMS value is located closer to the wall region. As the suction rate increases, the RMS value increases first, Then, at higher suction rates the maximum RMS value is reduced below the level recorded in experiments without suction. As the suction value further increases, one can expect that the RMS value in the boundary layer region will decrease to zero, and one will have a totally relaminarized a flow (figure 5). Unfortunately, with the existing equipment such large suction coefficients can not be obtained. But, as suggested by O. Brien (1965) relaminarization by suction slit doesn't seem to be the most effective way to obtain the reverse transition.

In view of the fact that relatively small suction values increase the momentum of the fluid close to the wall by a relatively large ratio, it would appear that a better method for relaminarization would be a distributed, relatively small quantity of suction.

At point B two inches upstream, on the other hand the profiles showed a relatively parallel shift. Local velocities augmented by a small constant amount. RMS values and their distribution did not show a significant change, as in the previous case at point A (Figure 5-6).

At point C four inches downstream the general pattern discusses above for point A remained valid with a small decrease in the efficiency of suction (fig.7-8). A dimensional plot of velocity versus the logarithm of the distance from the wall is also instructive in the sense that one can observe a departure from the well-known universal logarithmic relationship by the addition of curvature. This curvature increases with the increase in suction rates as indicated in Figure 10. Such profiles have been experimentally verified and are theoretically expected for uniform suction, as are the bilogarithmic profiles of Bradshaw (1966).

COMPUTED QUANTITIES.

To check the experimental procedure and to calibrate the overall system, velocity profiles without suction were compared to theoretical flat plate values. Friction velocity U_τ (UTAU) values were computed for the data points using a program based on a method developed by Powell (1965). This program determines a set of parameters for a given function which give the best least - square - fit to a given set of data points. About ten experimental points were used for such data fitting. The selection of the data points was done using an interactive computer program. The universal profile tested as the given function is:

$$\frac{U}{U_\tau} = \frac{1}{K} \left(\log \left(\frac{U_\tau y}{\nu}\right) + A\right) \quad ; \frac{1}{K} = 5.5 \text{ and } A/K = 5.45$$

The value of U_τ thus computed was then compared to theoretical values. A maximum variation of 5% difference between computed and theoretical values was observed. A typical plot of such profiles is given in figure 11. One can observe that for $40 < y^* < 500$ the profile is logarithmic, but a certain amount of derivation is observed for $y^* > 500$. This derivation might be due to variations in the outer flow.

After the system was checked for calibration, the classical boundary layer parameters as defined below were computed using a numerical integration technique. These quantities were also compared to the theorically predicted ones. Except for boundary layer thickness values all other parameters compared well with the theoretical ones. The parameters studied and their definitions are given below.

Displacement thickness $$\delta^* = \int_0^\delta \left(1 - \frac{u}{U}\right) dy \qquad (2)$$

Momentum thickness $$\theta = \int_0^\delta \left(1 - \frac{u}{U}\right)\frac{u}{U}\, dy \qquad (3)$$

Energy thickness $$\theta_E = \int_0^\delta \left(1 - \frac{u^2}{U^2}\right)\frac{u}{U}\, dy \qquad (4)$$

Form factor $$H = \frac{\delta^*}{\theta} \qquad (5)$$

These parameters were later calculated for different profiles with and without suction to determine the boundary layer regime and the effect of suction on these variables.

Friction velocity values for the flat plate with suction was also computed using a formulation suggested by Bradshaw, Ferris, Atwell. This equation is:

$$u = \frac{U_\tau}{K}\left(\ln \frac{U_\tau y}{\nu} + A\right) + \frac{U_\tau}{K}\left[\ln\left(\frac{4}{2}\left(\frac{\sqrt{1-z}-1}{\sqrt{1+z}+1}\right)\right) + 2\left(\sqrt{1+z}-1\right)\right] \qquad (6)$$

where $z = \alpha y/\tau_w$, $K = .4$, $A = 2$

This time U_τ and α values are computed using the previously mentioned computer program.

This equation is assumed to be valid for $\frac{U_\tau y}{\nu} > 40$.

After the calculation of U_τ the assumption was checked for validity. Direct measurement of the friction velocity would be highly desirable but the difficulties in the calibrations suggested this numerical procedure instead. Figures 12-14 show the effect of suction on the boundary layer profile. On the horizontal axes the logarithm of y* is plotted versus the nondimensionalized velocity for different suction parameters (S.P.), which is the estimated velocity at the slit in meters/sec. It is interesting to note that with this computational procedure the data collapse in the region $10 < y^* < 100$ but then begin to diverge part the point $y^* > 100$.

Finally, the parameters are nondimensionalized by dividing them by the corresponding parameter at zero suction and at the same Reynolds number. Figures 15 to 29 are plots of nondimensionalized parameters versus suction coefficient. From these diagrams the following can be conjectured.

1 - The logarithm of non dimensionalized displacement, momentum, and energy thickness show a linear dependence on the suction coefficient.

2 - The form factor remains almost constant at about 1.1 with a slight increase as the suction coefficient increases.

3 - The nondimensionalized friction velocity or shear stress also shows a logarithmic relationship to the suction coefficient.

For the boundary layer parameters the following relationships are then experimentally obtained.

$$\ln\left(\frac{\delta^* \text{ with suction}}{\delta^* \text{ without suction}}\right) = A_1 \cdot S_c + B_1 \qquad \text{7-a}$$

$$\ln\left(\frac{\theta \text{ with suction}}{\theta \text{ without suction}}\right) = A_2 \cdot S_c + B_2 \qquad \text{7-b}$$

$$\ln\left(\frac{\theta_e \text{ with suction}}{\theta \text{ without suction}}\right) = A_3 \cdot S_c + B_3 \qquad \text{7-c}$$

$$\ln\left(\frac{u_\tau \text{ with suction}}{u_\tau \text{ without suction}}\right) = A_4 S_c + B_4 \qquad \text{7-d}$$

The coefficients A_i are strongly dependent on the location with respect to suction slit and B_i is very close to 0. The values of A_i and B_i are obtained by applying a linear regression fit to the data and are given on the diagram as SLOPE and INTCP. One can easily see that the SLOPE values are in most cases reduced by a factor of 2 as one moves from the experiment point A to the experiment point C. The net effect of suction upstream is relatively weak compared to the effect downstream. (Figure 15-29)

DISCUSSION OF RESULTS

At all three test locations considered, boundary layer suction affected the boundary layer profiles. The effect is more pronounced downstream from the slit than upstream. Boundary layer suction increased the flow momentum close to the wall at the expense of increased skin friction. No complete empirical or theoretical curve can be given at this time, but the nondimensionalized boundary layer parameters are observed to be related primarily to the suction coefficient. The dependence on Reynolds number seems to be either a weak one or implicit in the parameters. Friction velocities are computed numerically. It is highly desirable that they also be verified experimentally. This will simplify experimentation procedures and also increase the confidence limit. The scatter of data is the result of experimental and numerical procedures, and seems to be within an acceptable range. The values given for slope and intercept should be used as trend curve and not as a design parameter. The "effectiveness" of suction downstream from the slit can be studied as a variation of the slope for the curve relating boundary layer parameters to the suction coefficient at different test locations.

At this point it seems that a frequency analysis of the fluctuating component of the velocity might give additional information as to its spectrum along with the variation of this spectrum when suction is used. This procedure will give a measure of the turbulent kinetic energy decay.

The effect of the pressure gradient away from the slit, resulting from slit suction is assumed in this work to be small. In ship model applications, on the other hand, one can not use the same assumption. It would therefore be necessary to include this parameter for a more general application.

CONCLUSIONS

Experiments were conducted over a relatively small range of Reynolds numbers $5x10^5<Re<1.1x10^6$. The maximum suction coefficient applied was $S_C= 3$. A detailed study of these experiments show that slit suction decreases the loss of momentum in the boundary layer at the expense of an increase of skin friction. A moderate suction rate can therefore be applied to retard or stop separation to decrease form resistance. At higher suction rates as the U_τ value increases both upstream and down stream from the slit location, additional increase in suction may not be beneficial from the point of view of resistance optimization. The range of the Renolds numbers covered in this experiment is not exactly the range of the previously mentioned experiments where suction was applied to the ship model. In that case the range of Reynolds numbers was 8.3×10^5 $Re<19 \times 10^5$. The maximum suction coefficient in the same experiments was $S_c = 1.9$. For the optimum suction value of about 5 gallons/min the corresponding coefficient was Sc = .5.

Using the results of the current experiments we can conclude that the resistance of a ship model or of a ship can be successfully decreased by controlling separation which can be accomplished by suction slits. Relaminarization of the flow on the other hand requires much larger amount of suction Sc> 3. if a suction slit is to be employed. One can conjecture, therefore, that in the experiments reported in Calisal(1972) the application of suction decreased the wake and the wake resistance by reducing separation. Meanwhile, skin friction continuously increased, at least close to the suction slit. This resulted in an increase of frictional resistance past a certain suction value the suspected relaminarization was therefore absent, and not responsible for the reduction in total drag. For a ship similar reduction in drag is possible. The scaling should be done at suction coefficient values, since this parameter seems to be the dominant one.

The usage of distributed slits or continuous suction becomes apparent, as the dependence between boundary layer parameters and the suction coefficient is non linear.

Additional insight can be obtained from a similar study at higher Reynolds numbers. From the present study it would seem that Reynolds number dependence is implicit in the boundary layer parameters.

The variation of boundary layer parameters with suction depends more strongly on the suction coefficient and the relative location with respect to the slit.

It is hoped that a numerical procedure can be developed for boundary layer flows with injection or suction using the insight gained by this study. Additional problems such that combine boundary layer suction, pressure gradient and the free surface can be studied profitably. Additional experimental research for the direct measurement of friction velocity and Reynolds numbers at higher range are also being considered.

BIBLIOGRAPHY

1. Black T. J., Sarnecki A. J. "The Turbulent Boundary layer with Suction or Injection." Aeronautical Research Council Reports and Memoranda R & M No. 3387, Her Majesty's Stationary Office 1965.

2. Bradshaw P. "Limits of Validity of the Bilogarithmic Velocity Profile in Turbulent Boundary Layers with Suction or Injection." NPL AERO Report 1216, Nov 1966.

3. Bradshaw P., Ferriss D. H., Atwell N.P., "Calculation of Boundary-Layer Development using the Turbulent Energy Equation." NPL Aero Report 1182 Jan. 1966.

4. Bradshaw "A note on reverse transition". Journal of Fluid Mechanics (1969) vol. 35 part 2 pp 387-390

5. Calisal S. M. "Effect of wake on Wave Resistance", Journal of Ship Research, Vol 16, No 2, June, 1972, pp 303-307.

6. O'brien R. L. "Laminarization of Nozzle wall Boundary layers as a means of reducing heat flux." Technical Documentary Report No AFRPL - TR - 65 -40 February 1965. United Aircraft Research Laboratories.

7. Patel V. C., Head Mr. R. "Reversion of Turbulent to laminar flow." Journal of Fluid Mechanics (1968) Vol 34 part 2 pp 371-392

8. Powell, M. J. D. "A Method for Minimizing a Sum of Squares of Non-Linear Functions without Calculating Derivatives." The Computer Journal, January 1965 pp. 303-307 Vol 7.

9. Tennekes H. "Similarity laws for Turbulent boundary layers with suction or injection" Journal of Fluid Mechanics 1965 vol 21 part 4, pp 689-703.

10. Notes on "Lecture/Laboratory Primer on Turbulence" DISA Short course August 1976, U. S. Naval Academy, Annapolis, Maryland.

Acknowledgements

This work was sponsored by a Research grant of the Naval Academy Research Council.

The author is indebted to Miss C. Wroten for her effort in preparing the manuscript.

Initial Distribution List

		No. Copies
1.	Defense Documentation Center Cameron Station Alexandria, Virginia 22314	20
2.	Assistant Librarian Technical Processing Division U. S. Naval Academy Annapolis, Maryland 21402	4
3.	Department Chairman Department of Naval Systems Engineering U. S. Naval Academy Annapolis, Maryland 21402	2
4.	Division Director Division of Engineering and Weapons U. S. Naval Academy Annapolis, Maryland 21402	1
5.	Director of Research U. S. Naval Academy Annapolis, Maryland 21402	1
6.	Academic Dean U. S. Naval Academy Annapolis, Maryland 21402	1
7.	Prof. J. V. Wehausen Naval Architecture Department University of California, Berkeley California 94720	1

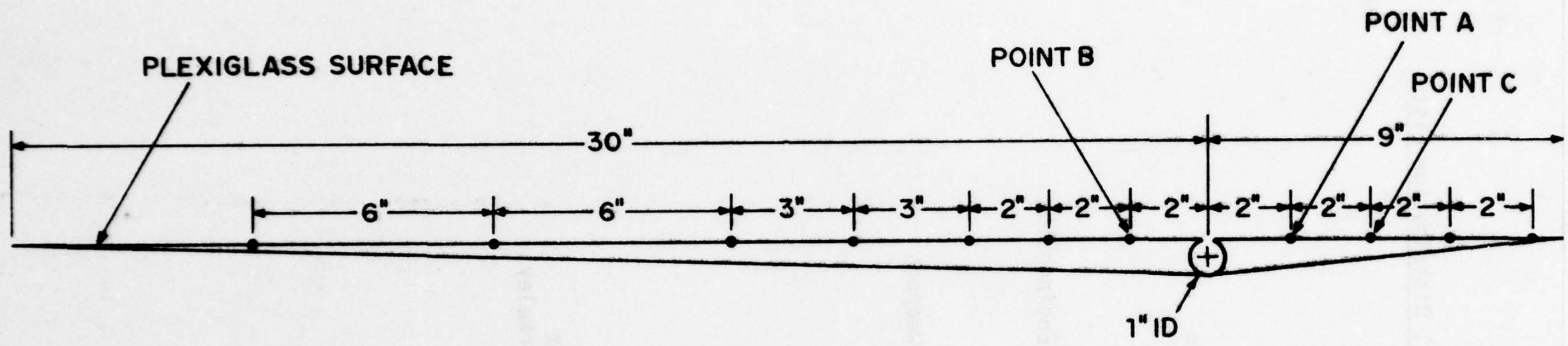

FIGURE 1 - MODEL AND THE LOCATION OF PRESSURE TAPS

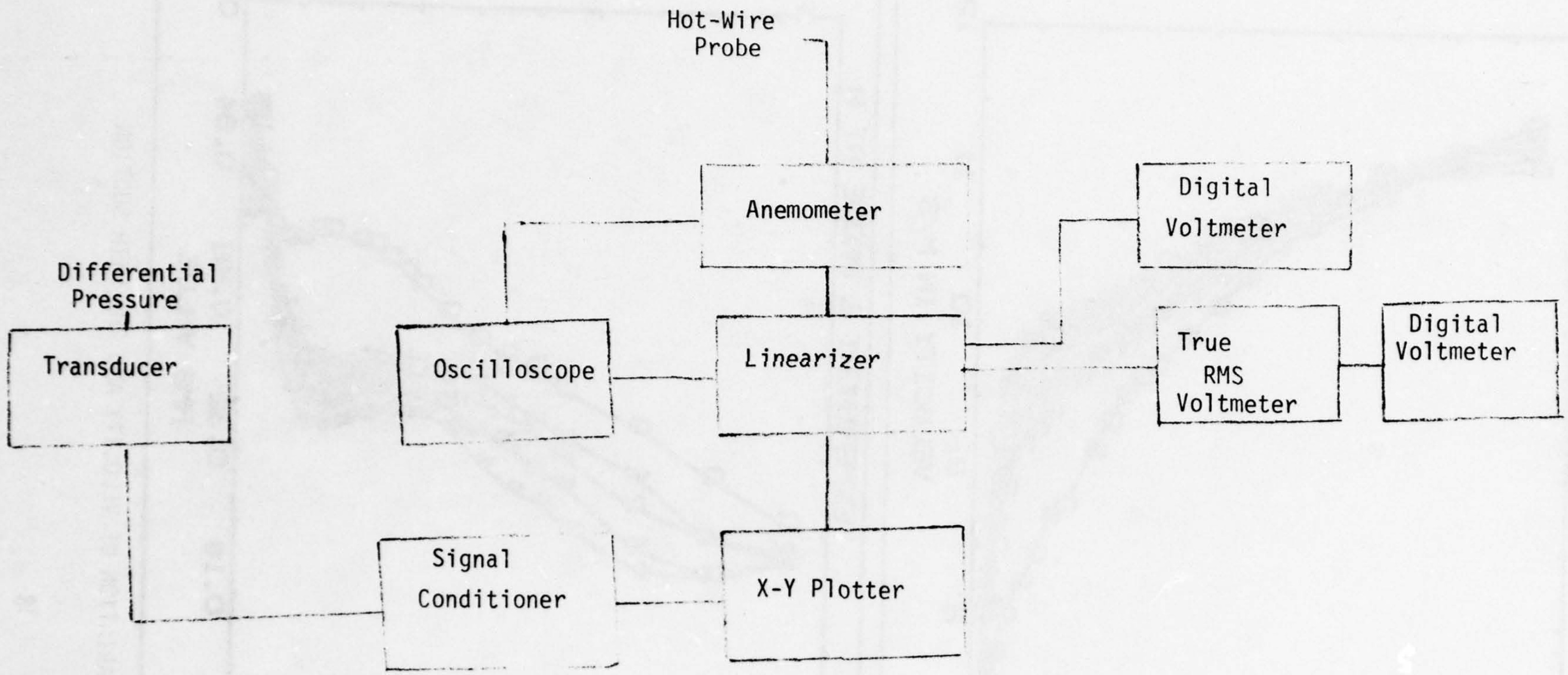

Calibration and Data Acquisition System for Hot Wire Probe

Figure 2

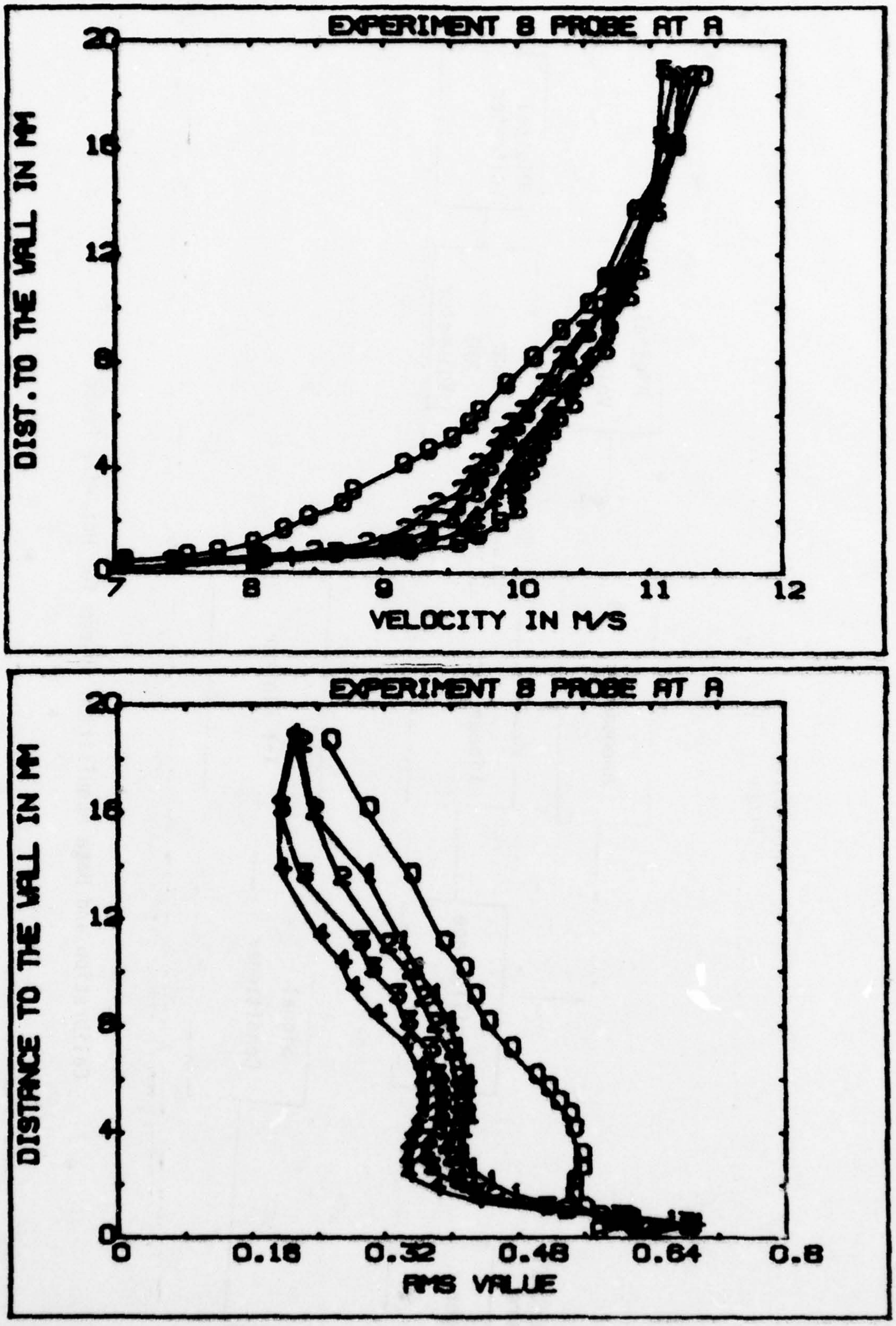

FIGURE 3-4 VARIATION OF VELOCITY AND RMS WITH SUCTION.

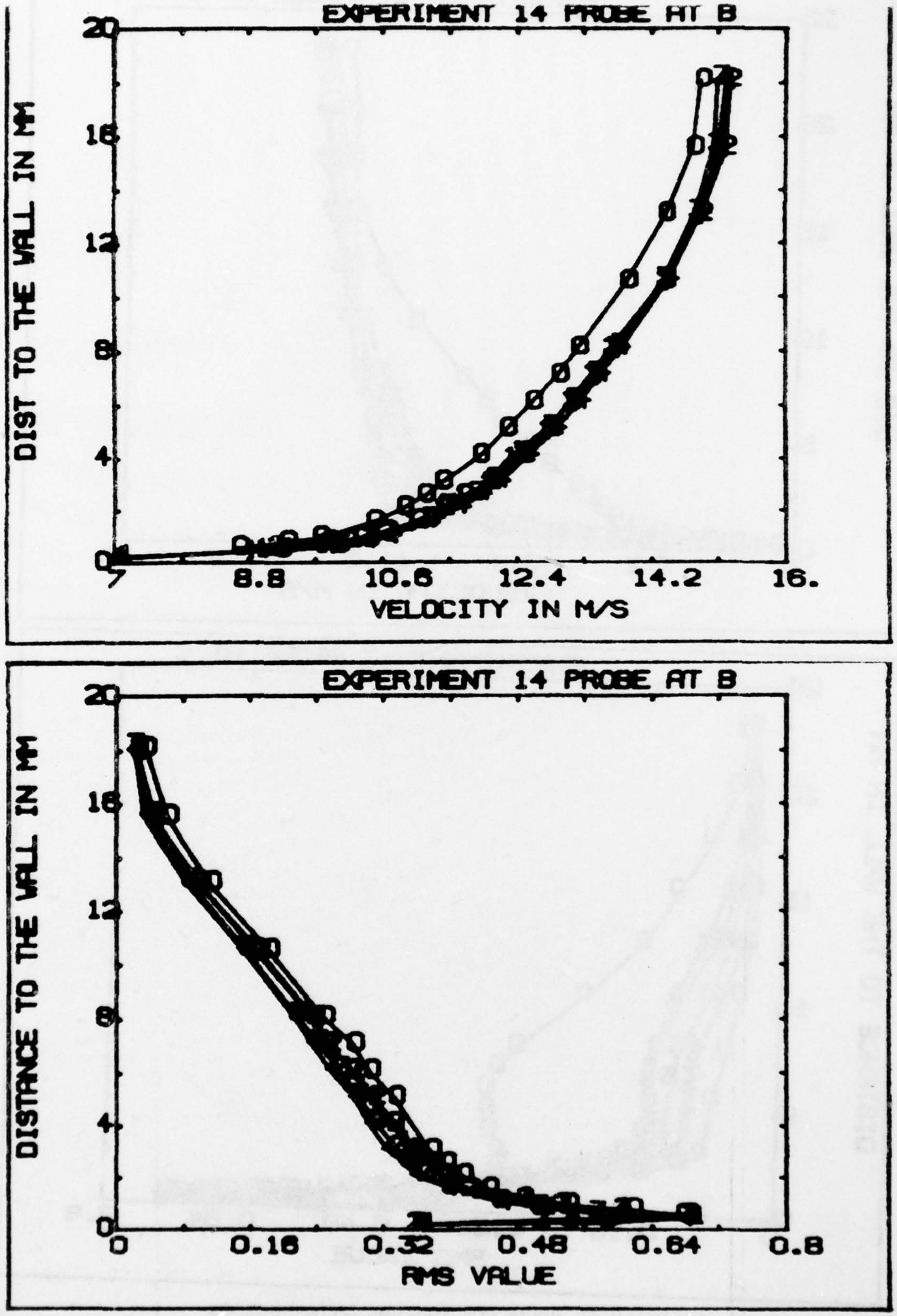

FIGURE 5-6 VARIATION OF VELOCITY AND RMS WITH SUCTION.

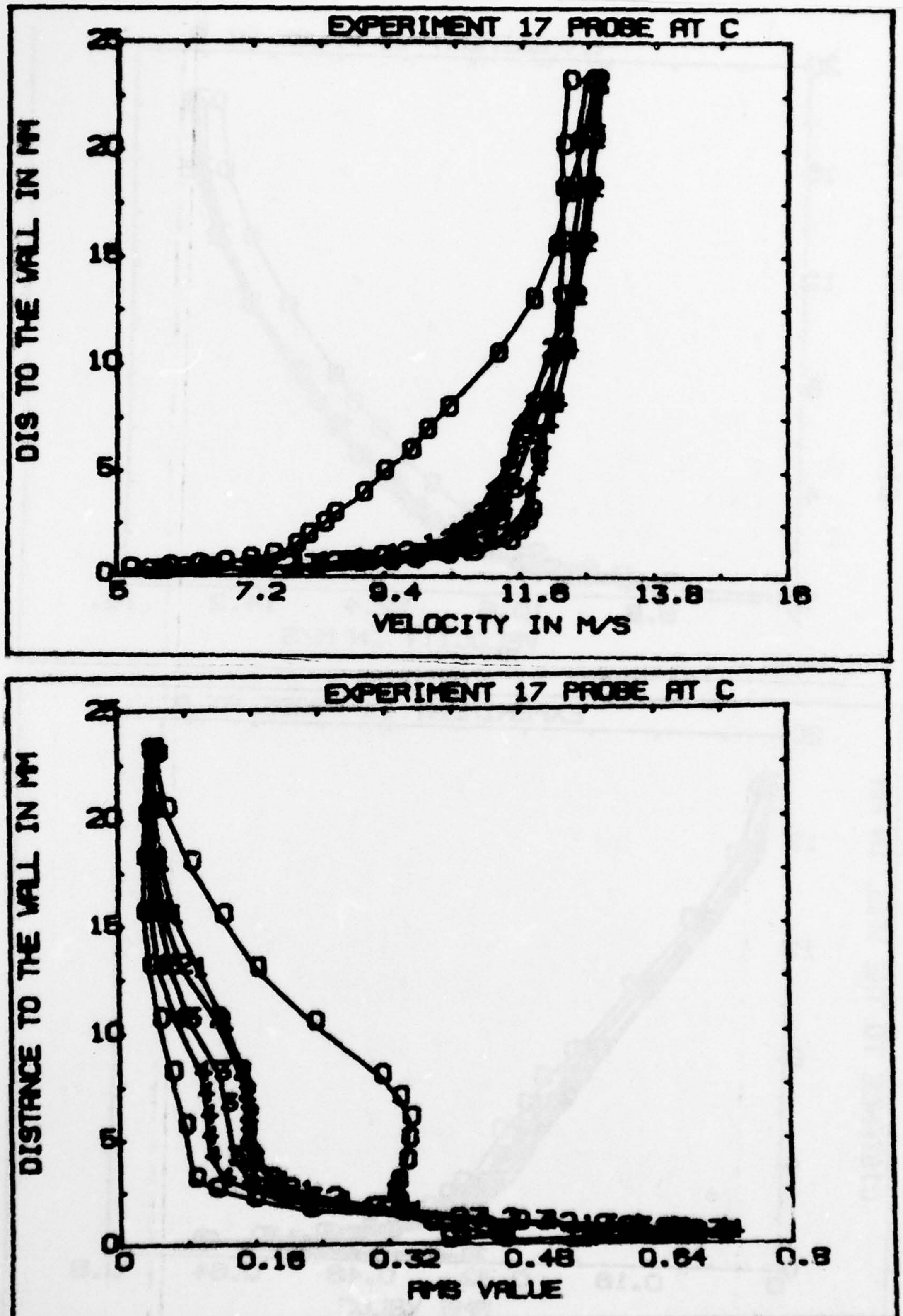

FIGURE 7-8 VARIATION OF VELOCITY AND RMS WITH SUCTION.

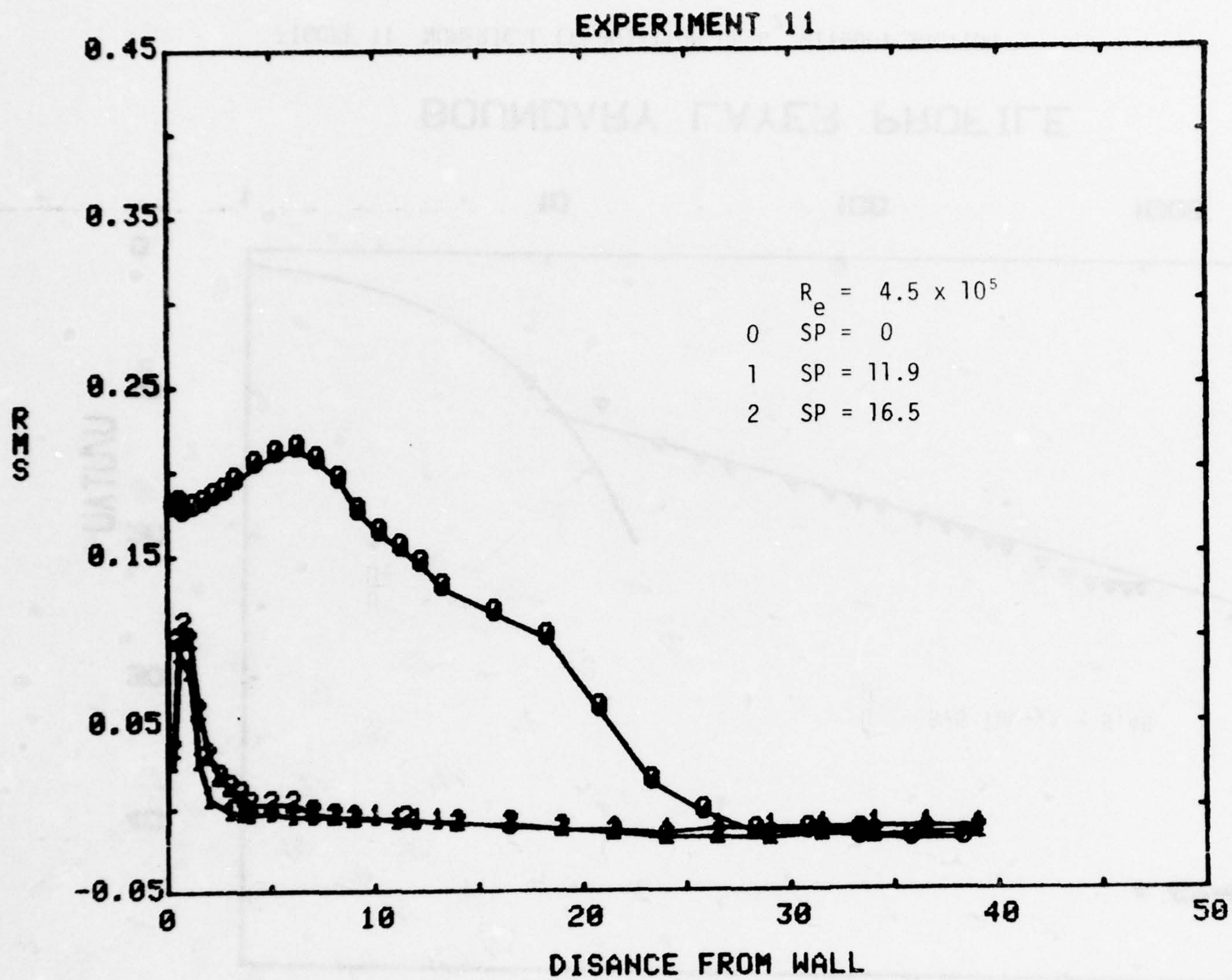

FIGURE 9 VARIATION OF RMS AT HIGH SUCTION VALVES

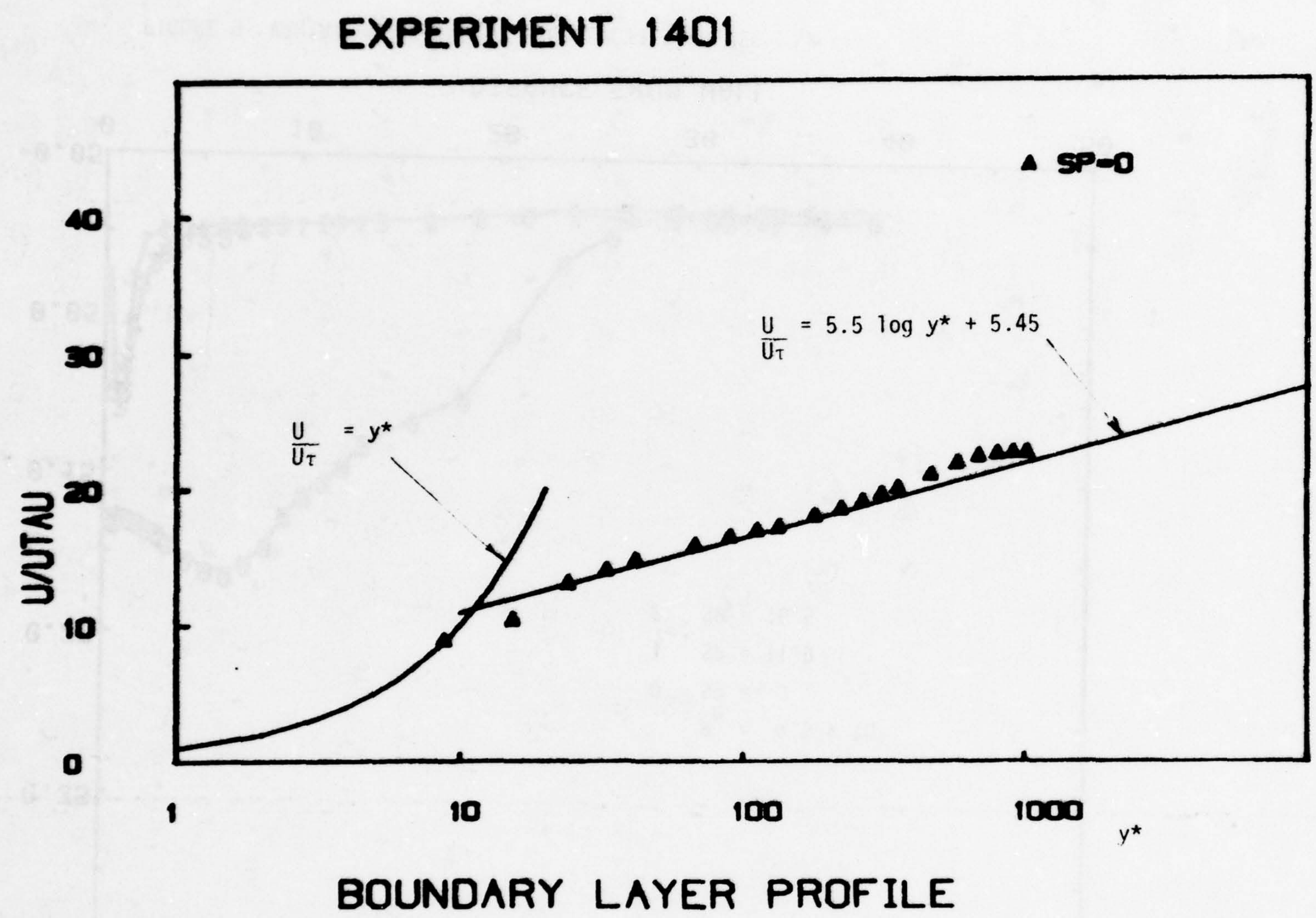

FIGURE 11 NUMERICAL COMPUTATION OF U_z WITHOUT SUCTION

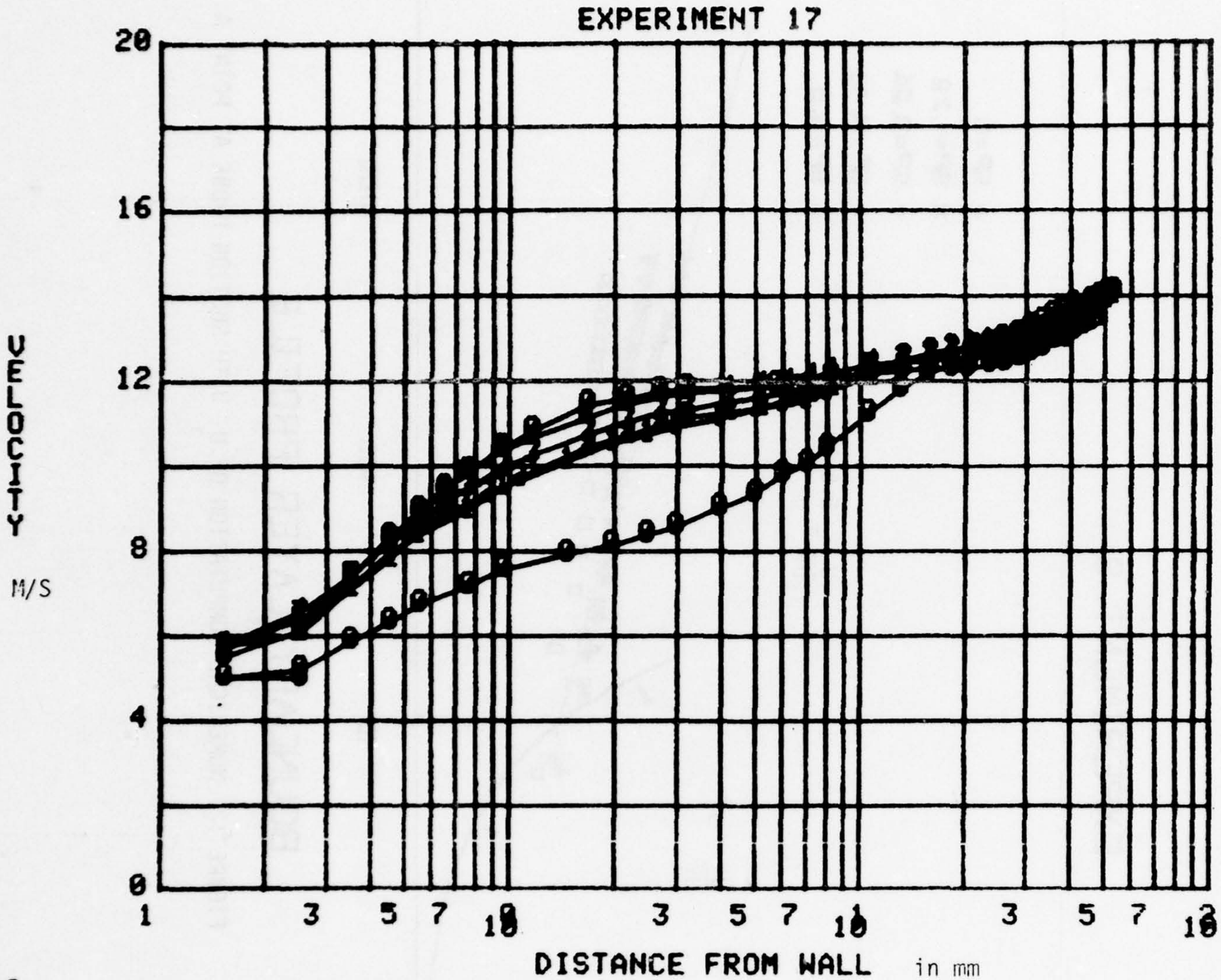

FIGURE 10 DIMENSIONAL PLOT OF VELOCITY VERSUS DISTANCE FROM THE WALL

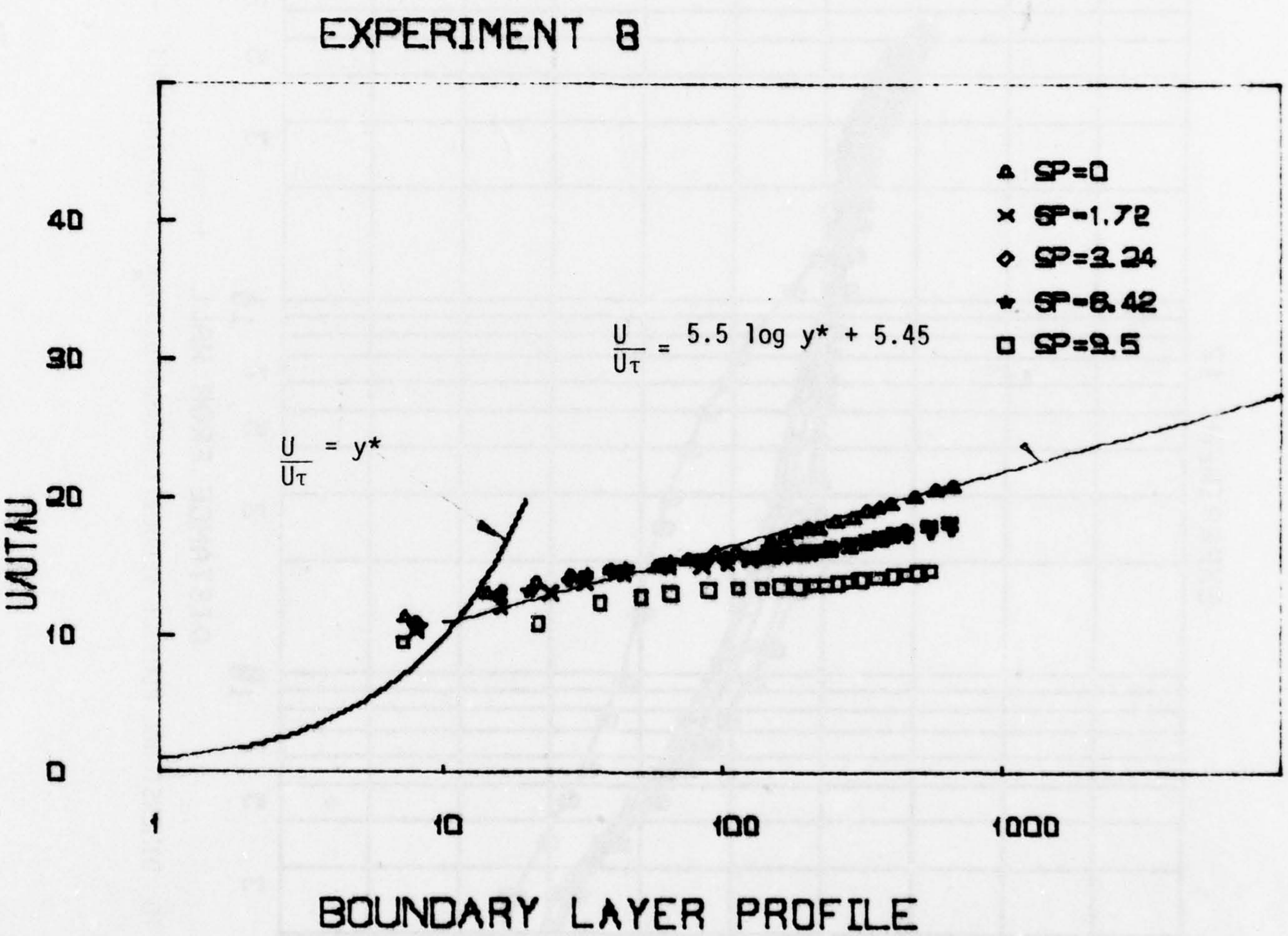

FIGURE 12 NUMERICAL COMPUTATION OF U_τ WITH SUCTION PROBE AT POINT A

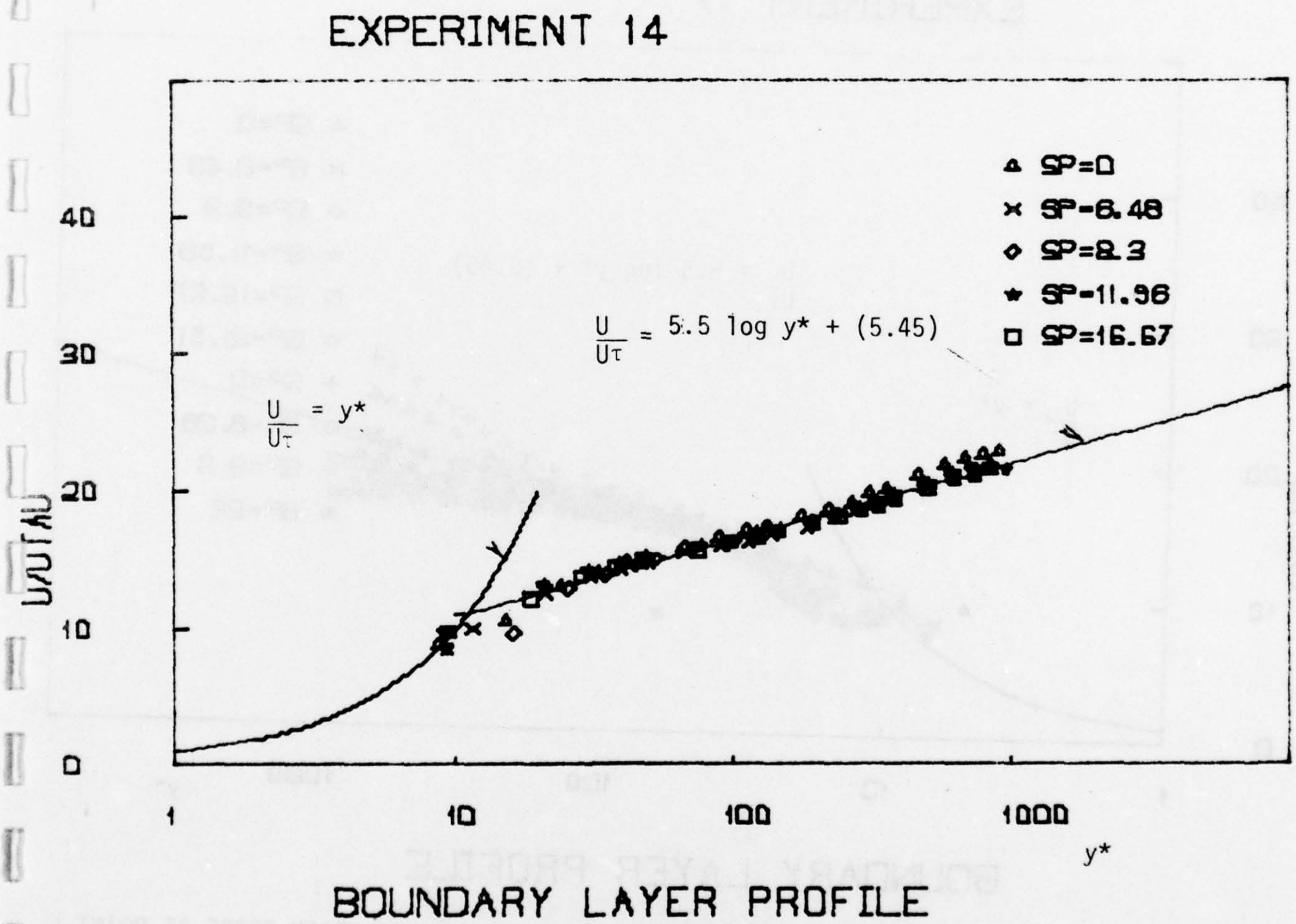

FIGURE 13 NUMERICAL COMPUTATION OF U_τ WITH SUCTION PROBE AT POINT B

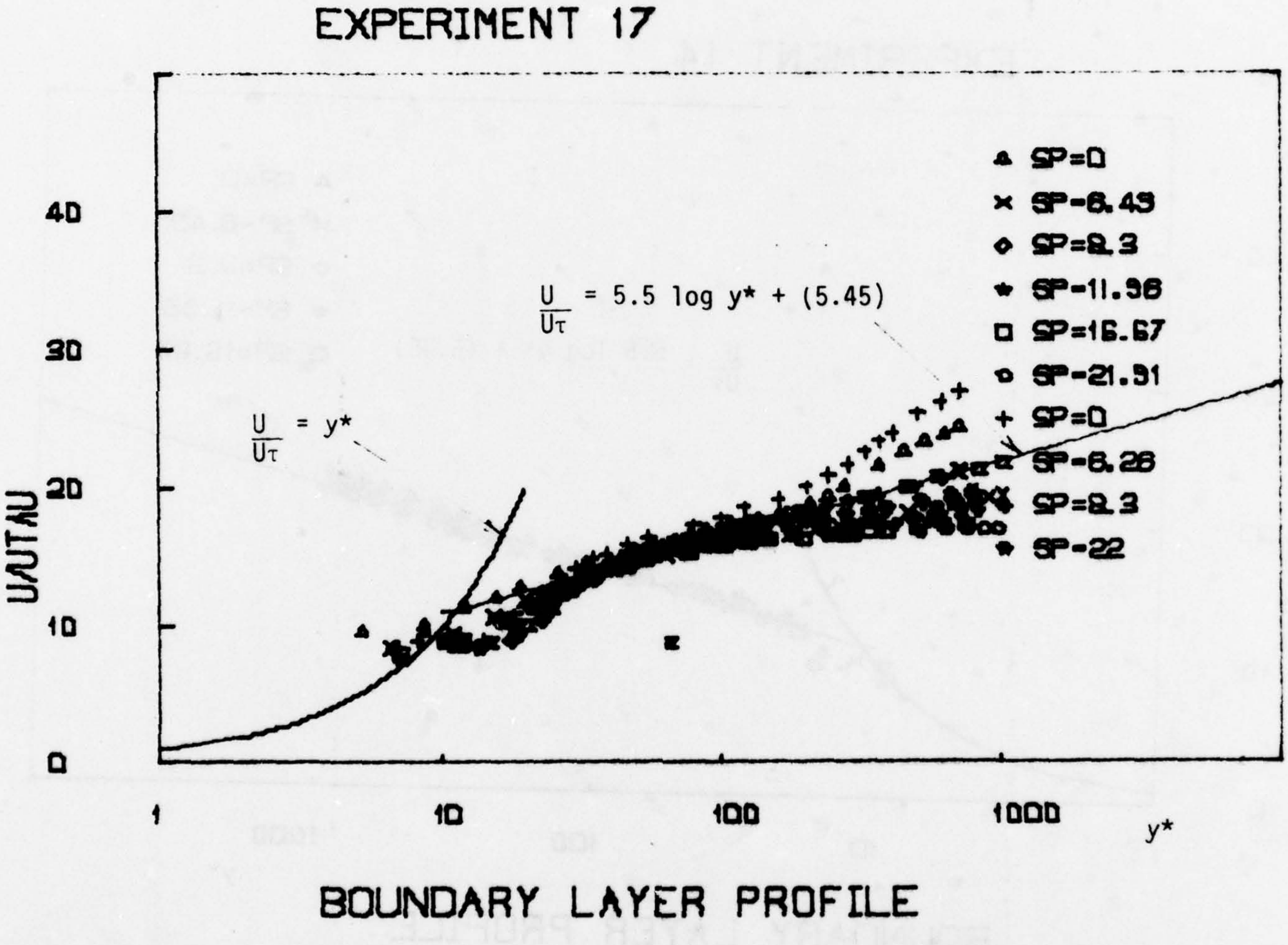

FIGURE 14 NUMERICAL COMPUTATION OF U_τ WITH SUCTION PROBE AT POINT C

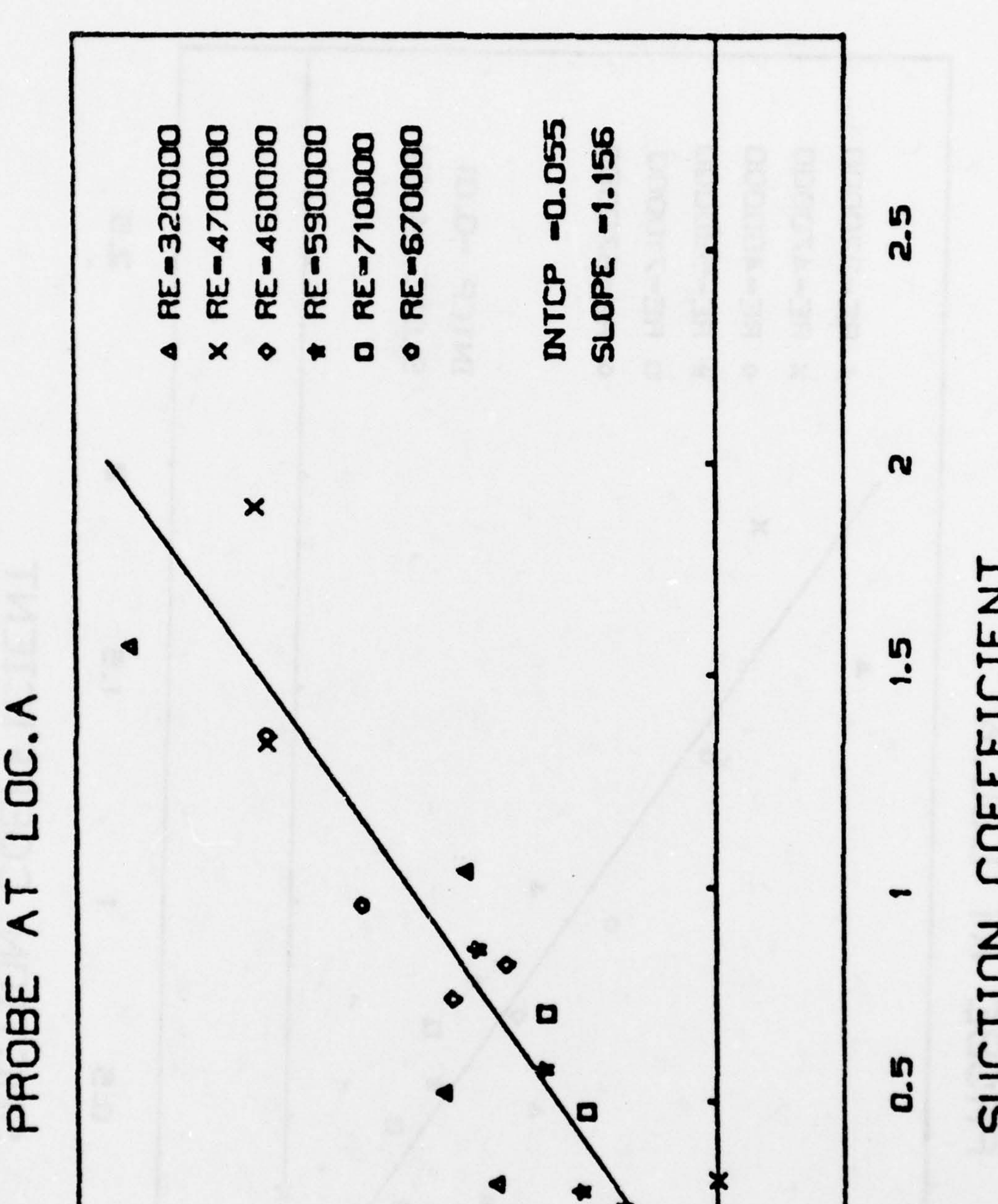
PROBE AT LOC.A
RE=320000
RE=470000
RE=460000
RE=590000
RE=710000
RE=670000
INTCP =0.055
SLOPE =1.156
LN OF NONDIM.DISP THICKNESS
7.3
4.4
2.7
1.6
1
0.6
SUCTION COEFFICIENT
0
0.5
1
1.5
2
2.5

FIGURE 15

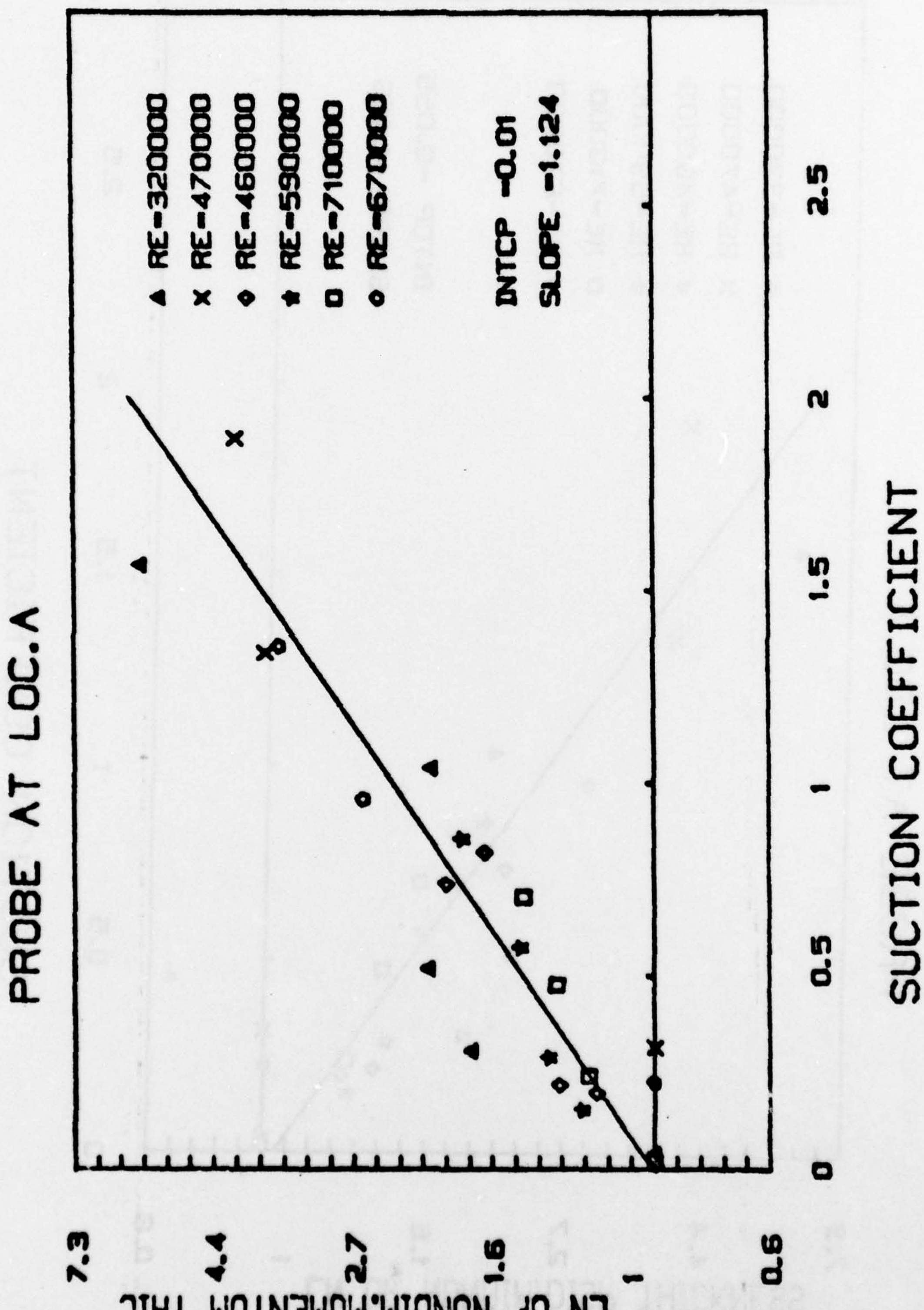
PROBE AT LOC.A
RE=3200000
RE=4700000
RE=4600000
RE=5900000
RE=7100000
RE=6700000
INTCP =0.01
SLOPE =1.124
7.3
4.4
2.7
1.6
1
0.6
0
0.5
1
1.5
2
2.5
LN OF NONDIM,MOMENTUM THIC
SUCTION COEFFICIENT

FIGURE 16

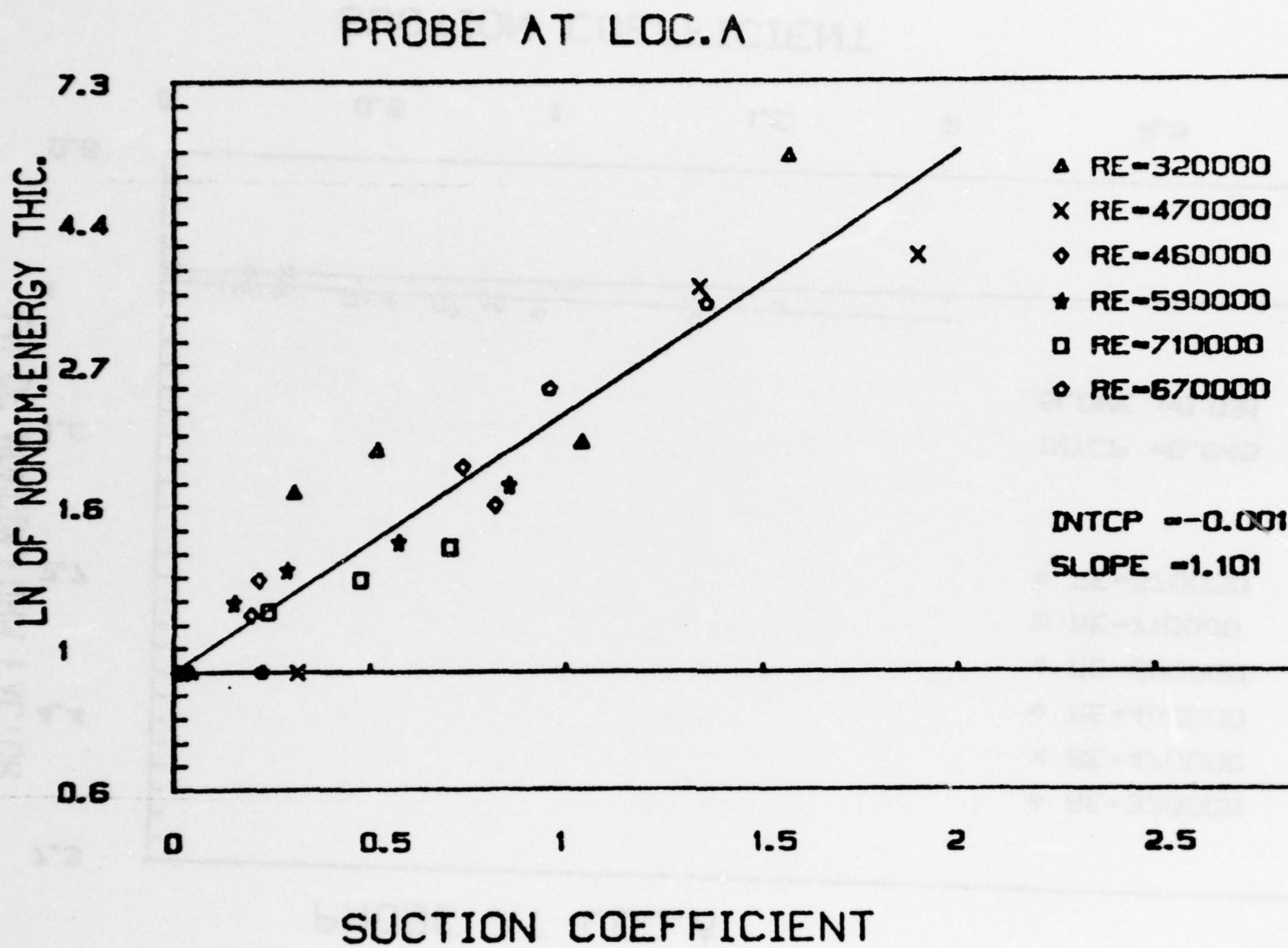
PROBE AT LOC.A
LN OF NONDIM.ENERGY THIC.
7.3
4.4
2.7
1.6
1
0.6
0
0.5
1
1.5
2
2.5
RE=320000
RE=470000
RE=460000
RE=590000
RE=710000
RE=670000
INTCP =-0.001
SLOPE =1.101
SUCTION COEFFICIENT

FIGURE 17

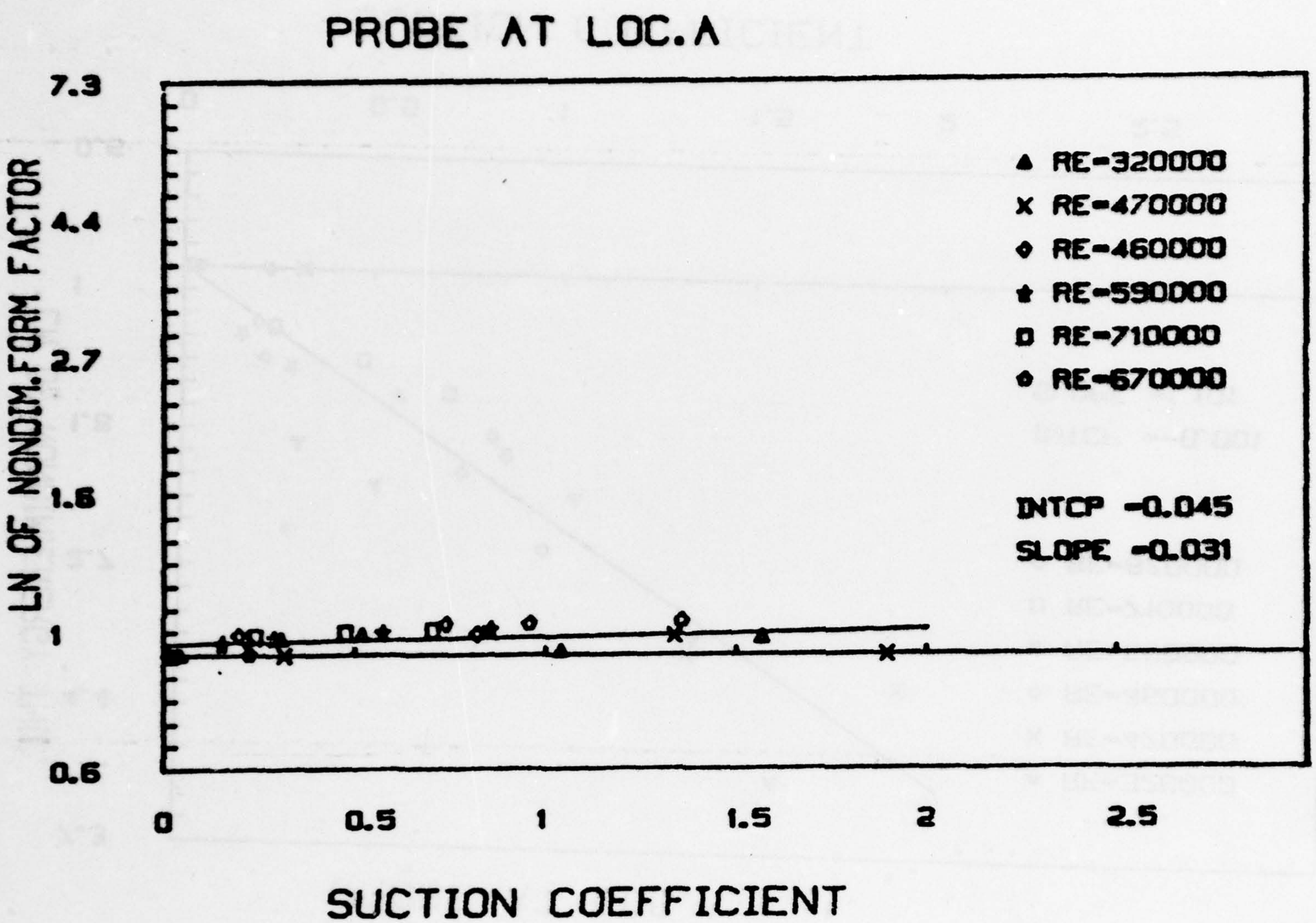
PROBE AT LOC.A
7.3
4.4
2.7
1.6
1
0.6
LN OF NONDIM.FORM FACTOR
0
0.5
1
1.5
2
2.5
SUCTION COEFFICIENT
RE=320000
RE=470000
RE=460000
RE=590000
RE=710000
RE=670000
INTCP -0.045
SLOPE -0.031

FIGURE 18

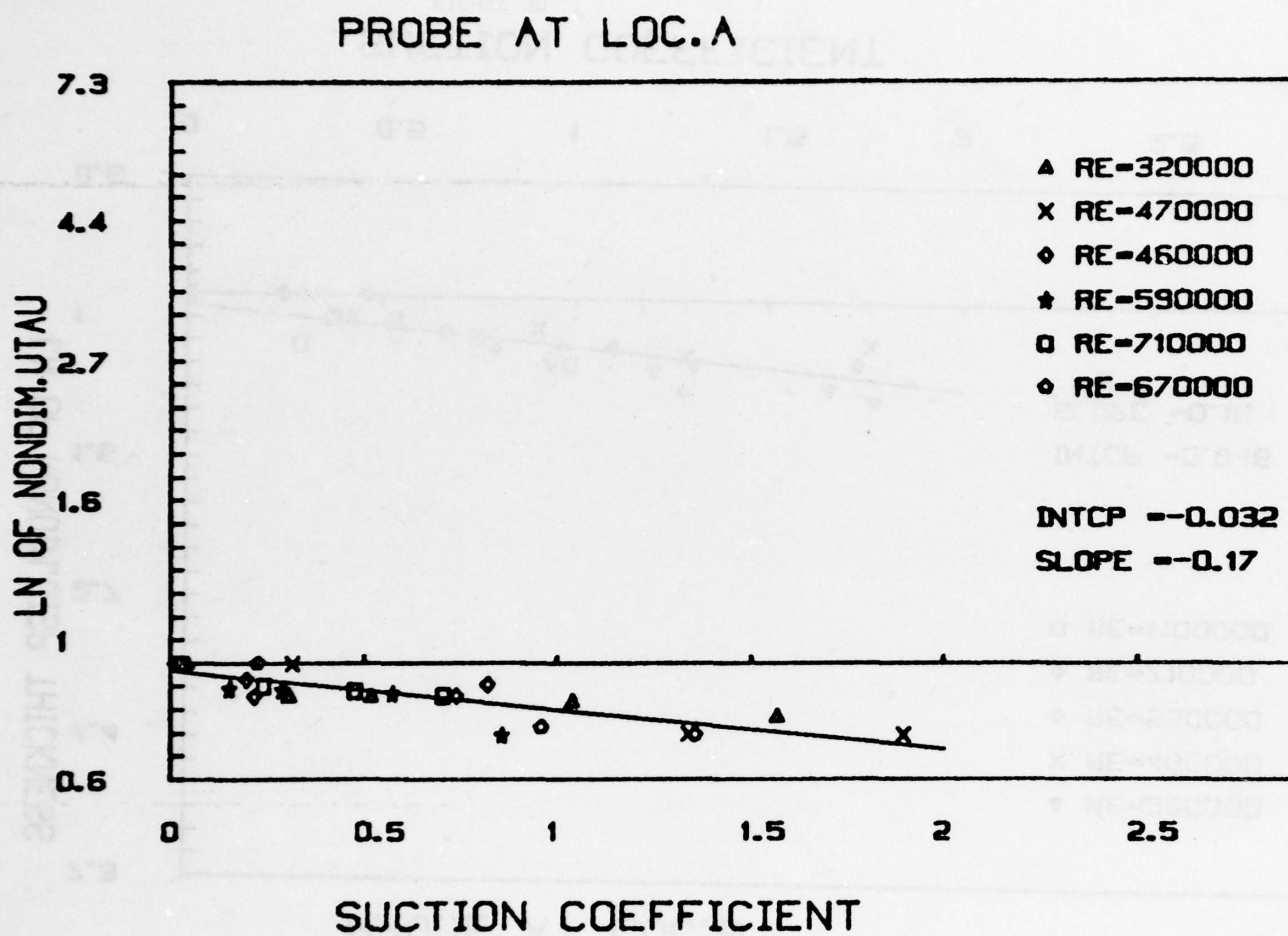

PROBE AT LOC.A
7.3
4.4
2.7
1.6
1
0.6
LN OF NONDIM.UTAU
0
0.5
1
1.5
2
2.5
SUCTION COEFFICIENT
RE=320000
RE=470000
RE=460000
RE=590000
RE=710000
RE=670000
INTCP =-0.032
SLOPE =-0.17

FIGURE 19

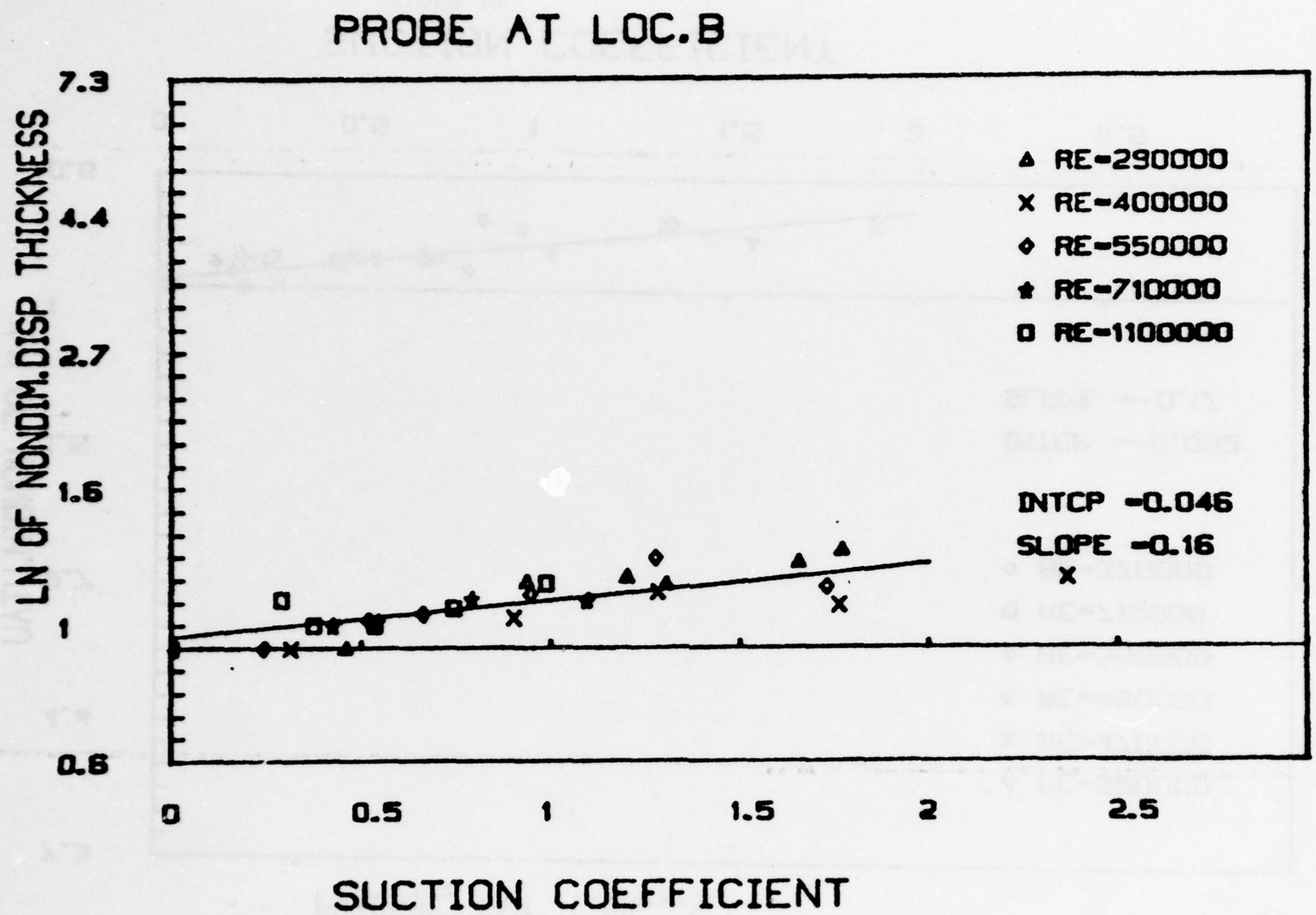

PROBE AT LOC.B
LN OF NONDIM.DISP THICKNESS
7.3
4.4
2.7
1.6
1
0.8
0
0.5
1
1.5
2
2.5
RE=290000
RE=400000
RE=550000
RE=710000
RE=1100000
INTCP =0.046
SLOPE =0.16
X
SUCTION COEFFICIENT

FIGURE 20

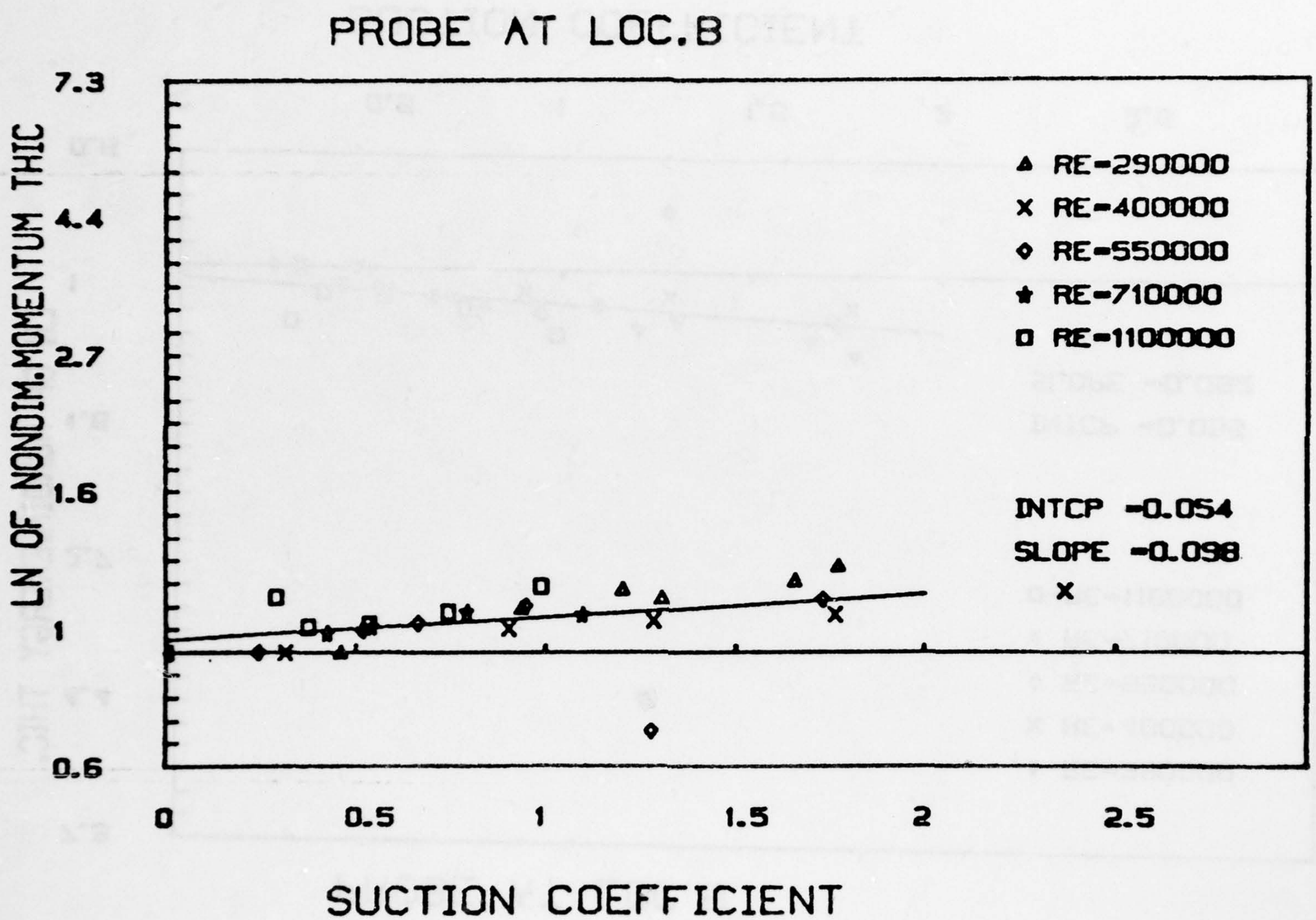
PROBE AT LOC.B
LN OF NONDIM.MOMENTUM THIC
7.3
4.4
2.7
1.6
1
0.6
0
0.5
1
1.5
2
2.5
SUCTION COEFFICIENT
RE=290000
RE=400000
RE=550000
RE=710000
RE=1100000
INTCP =0.054
SLOPE =0.098

FIGURE 21

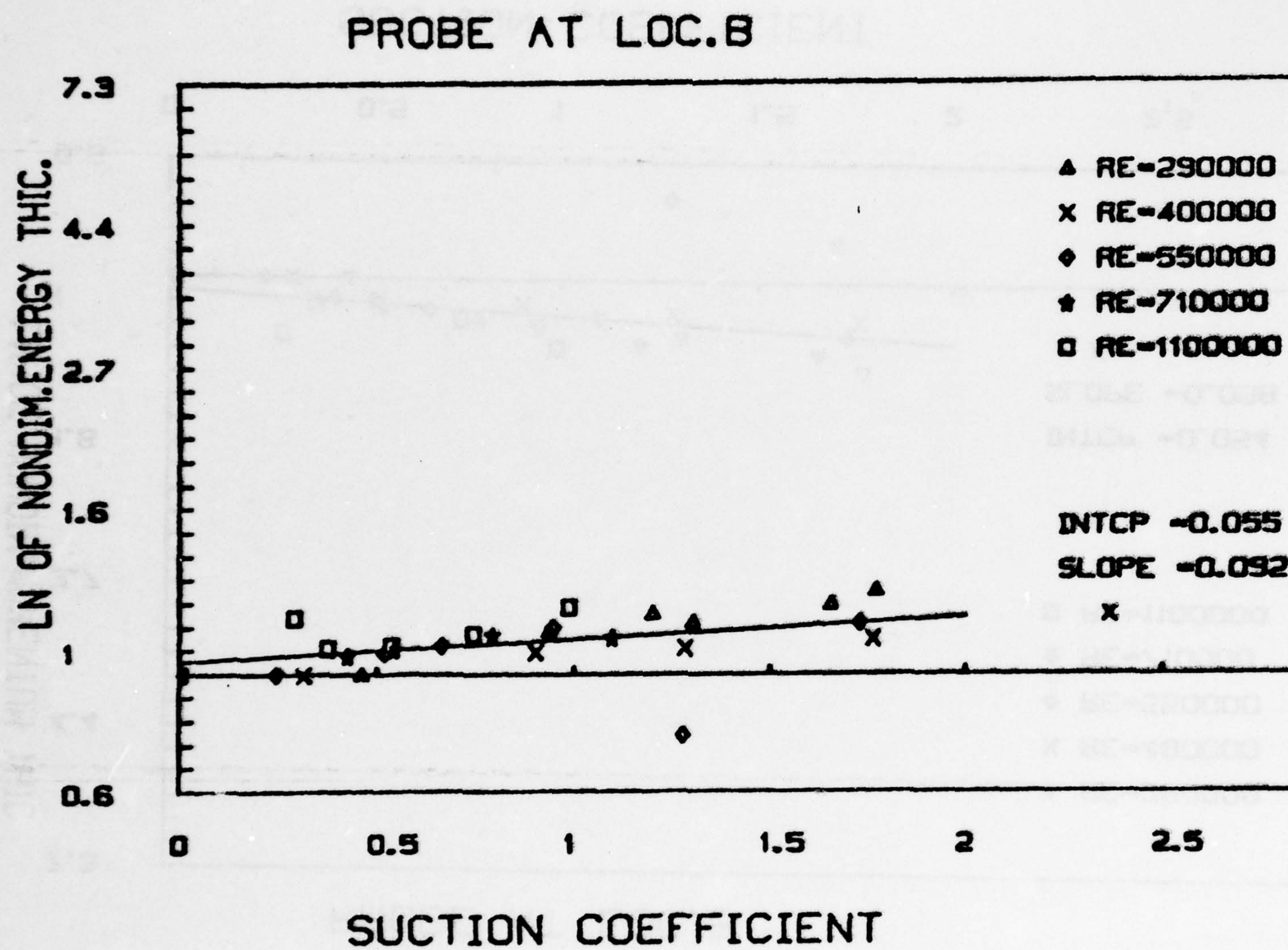
PROBE AT LOC.B
LN OF NONDIM.ENERGY THIC.
7.3
4.4
2.7
1.6
1
0.6
0
0.5
1
1.5
2
2.5
RE=290000
RE=400000
RE=550000
RE=710000
RE=1100000
INTCP =0.055
SLOPE =0.092
SUCTION COEFFICIENT

FIGURE 22

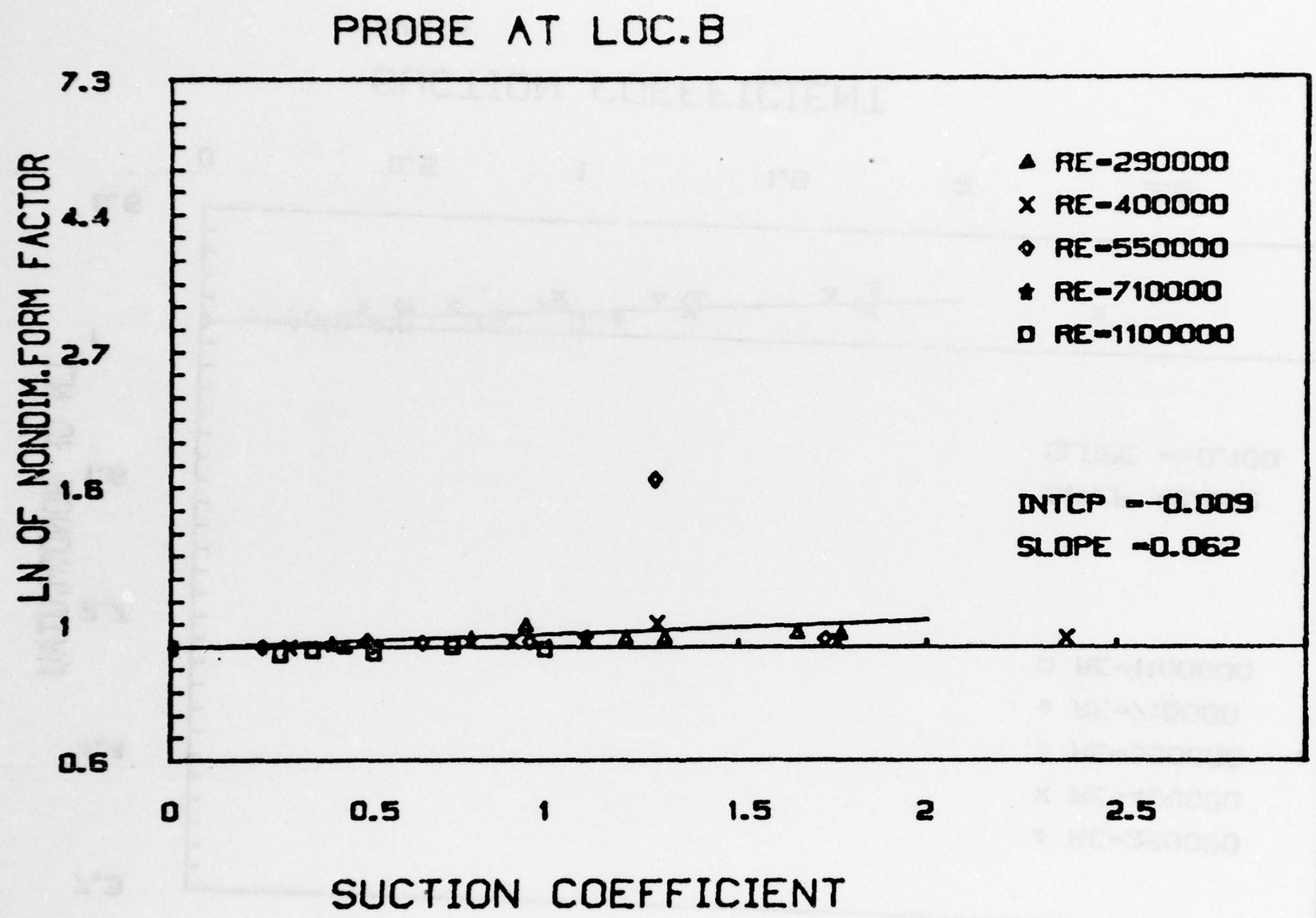

PROBE AT LOC.B
LN OF NONDIM.FORM FACTOR
7.3
4.4
2.7
1.8
1
0.6
0
0.5
1
1.5
2
2.5
RE=290000
RE=400000
RE=550000
RE=710000
RE=1100000
INTCP =-0.009
SLOPE =0.062
SUCTION COEFFICIENT

FIGURE 23

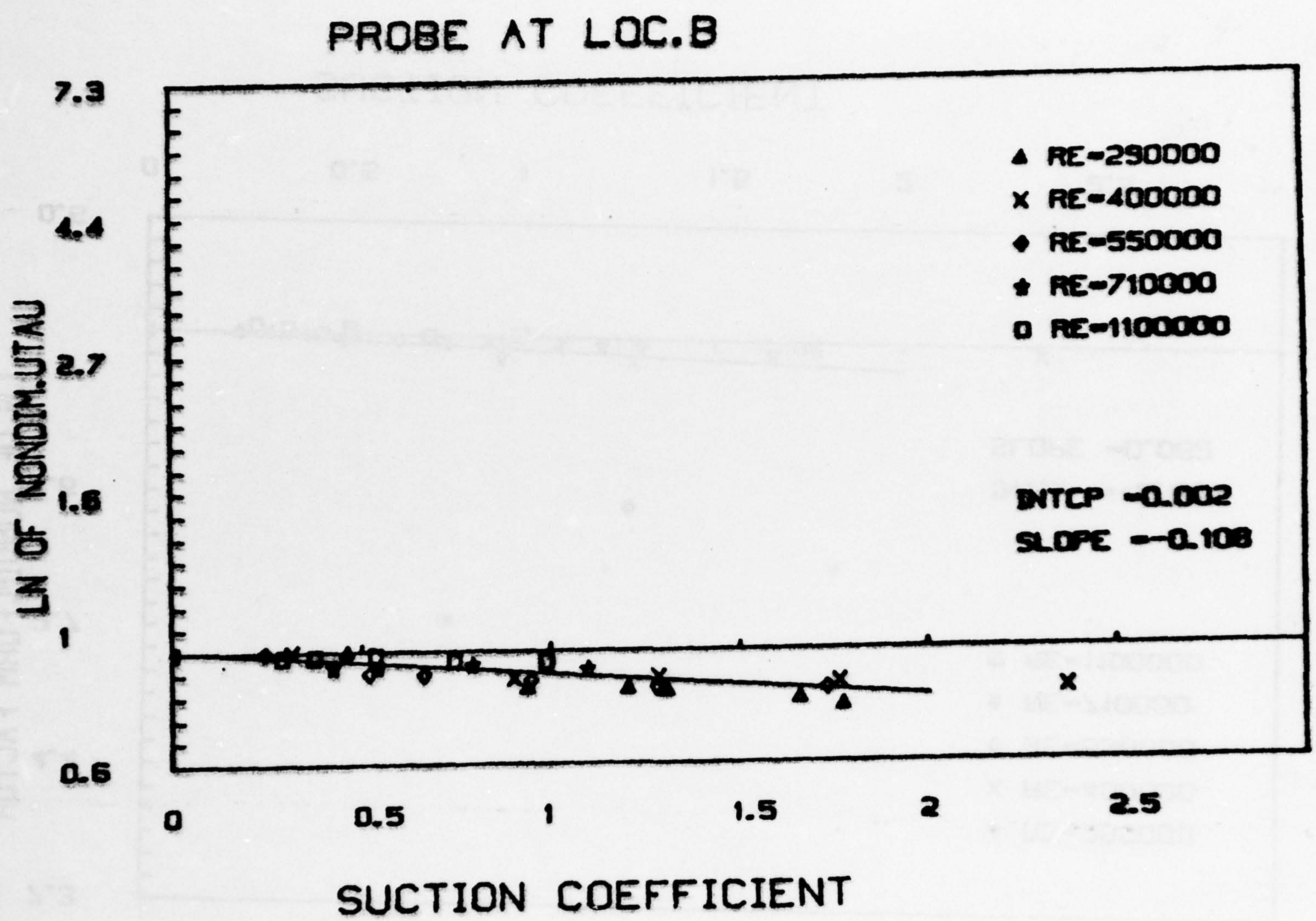
PROBE AT LOC.B
7.3
4.4
2.7
1.6
1
0.6
LN OF NONDIM.UTAU
0
0.5
1
1.5
2
2.5
SUCTION COEFFICIENT
RE=290000
RE=400000
RE=550000
RE=710000
RE=1100000
INTCP =0.002
SLOPE =-0.108

FIGURE 24

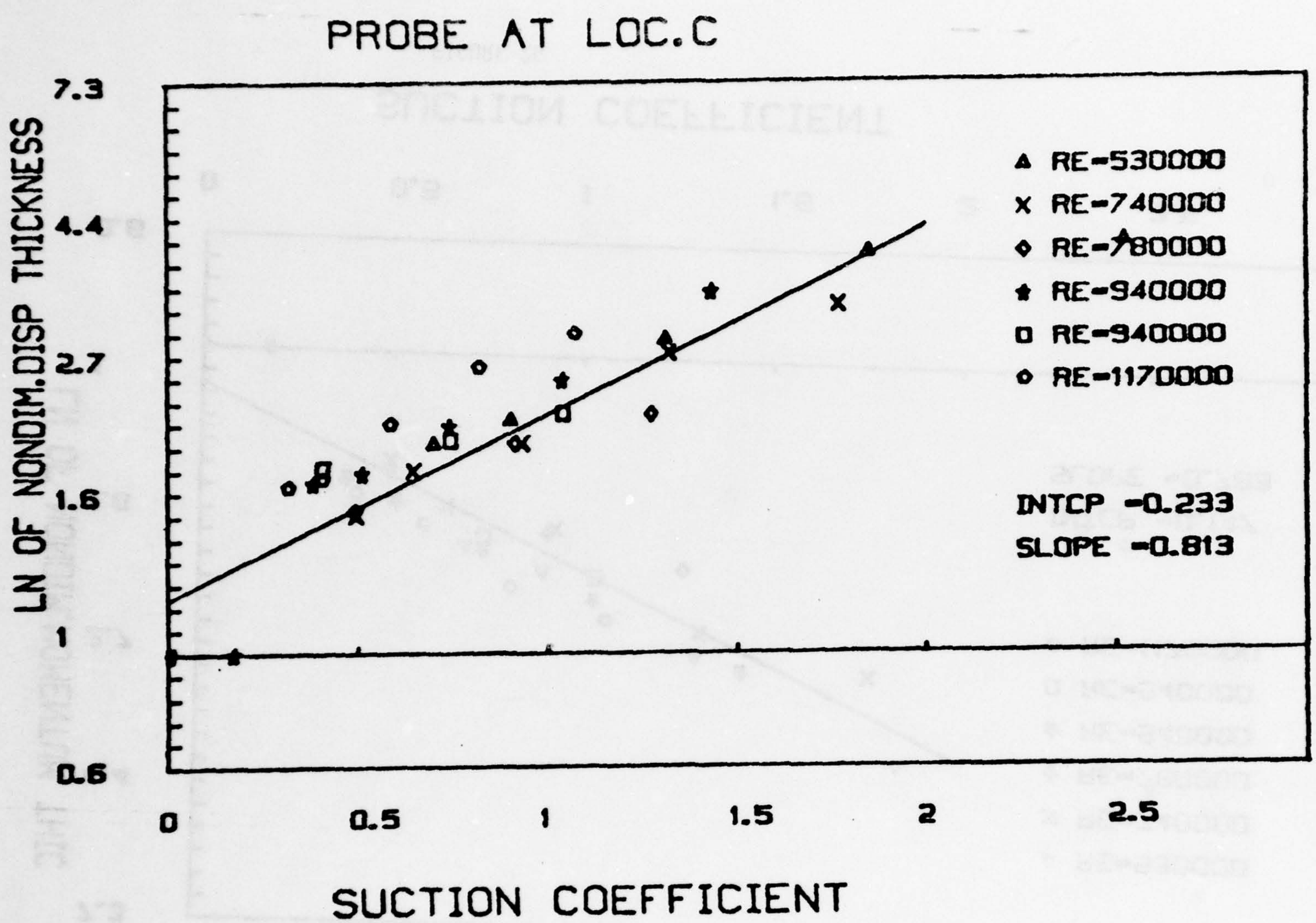

PROBE AT LOC.C
LN OF NONDIM.DISP THICKNESS
7.3
4.4
2.7
1.6
1
0.6
0
0.5
1
1.5
2
2.5
SUCTION COEFFICIENT
RE=530000
RE=740000
RE=780000
RE=940000
RE=940000
RE=1170000
INTCP =0.233
SLOPE =0.813

FIGURE 25

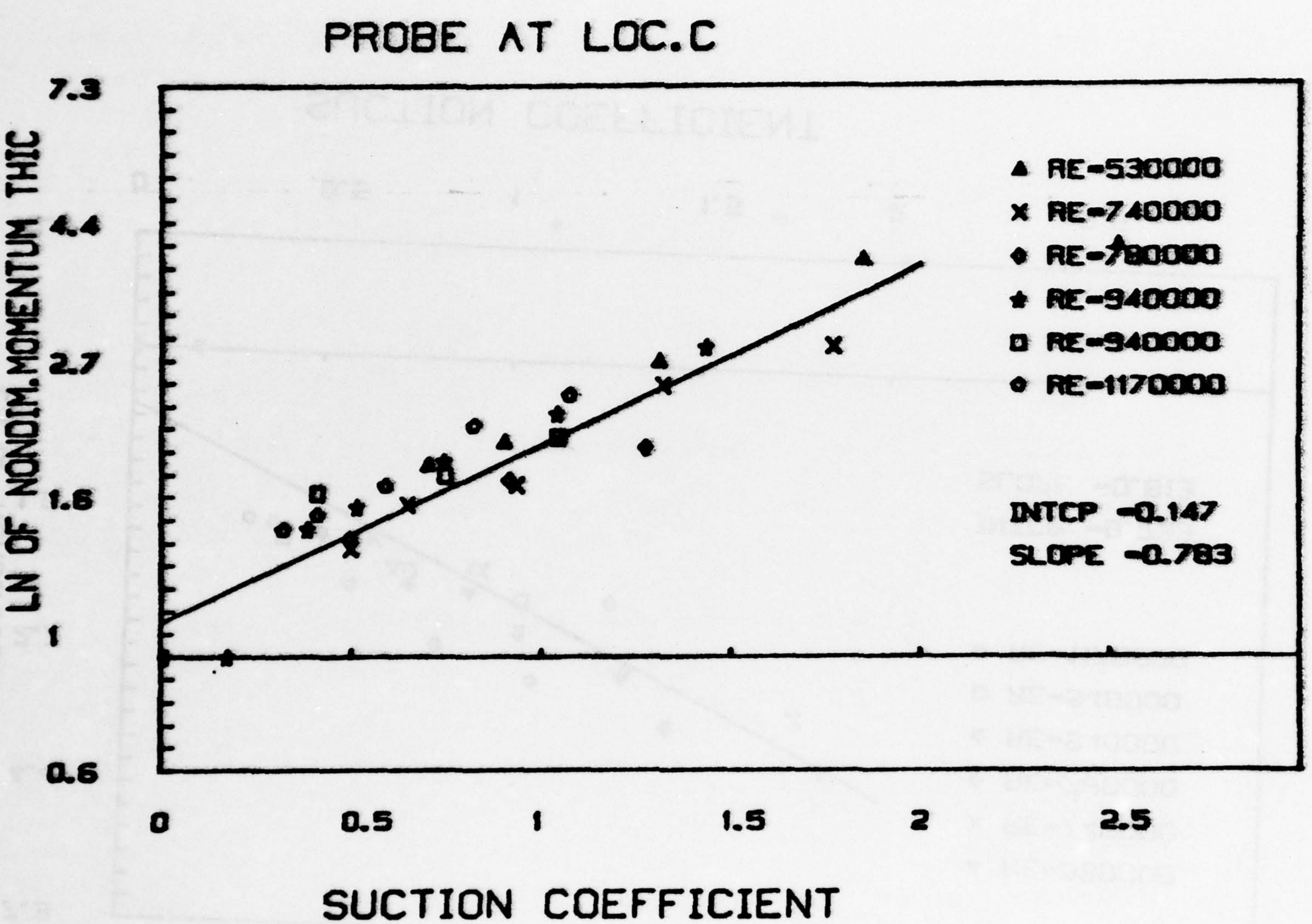
PROBE AT LOC.C
LN OF NONDIM.MOMENTUM THIC
7.3
4.4
2.7
1.6
1
0.6
0
0.5
1
1.5
2
2.5
SUCTION COEFFICIENT
RE-530000
RE-740000
RE-780000
RE-940000
RE-940000
RE-1170000
INTCP -0.147
SLOPE -0.783

FIGURE 26

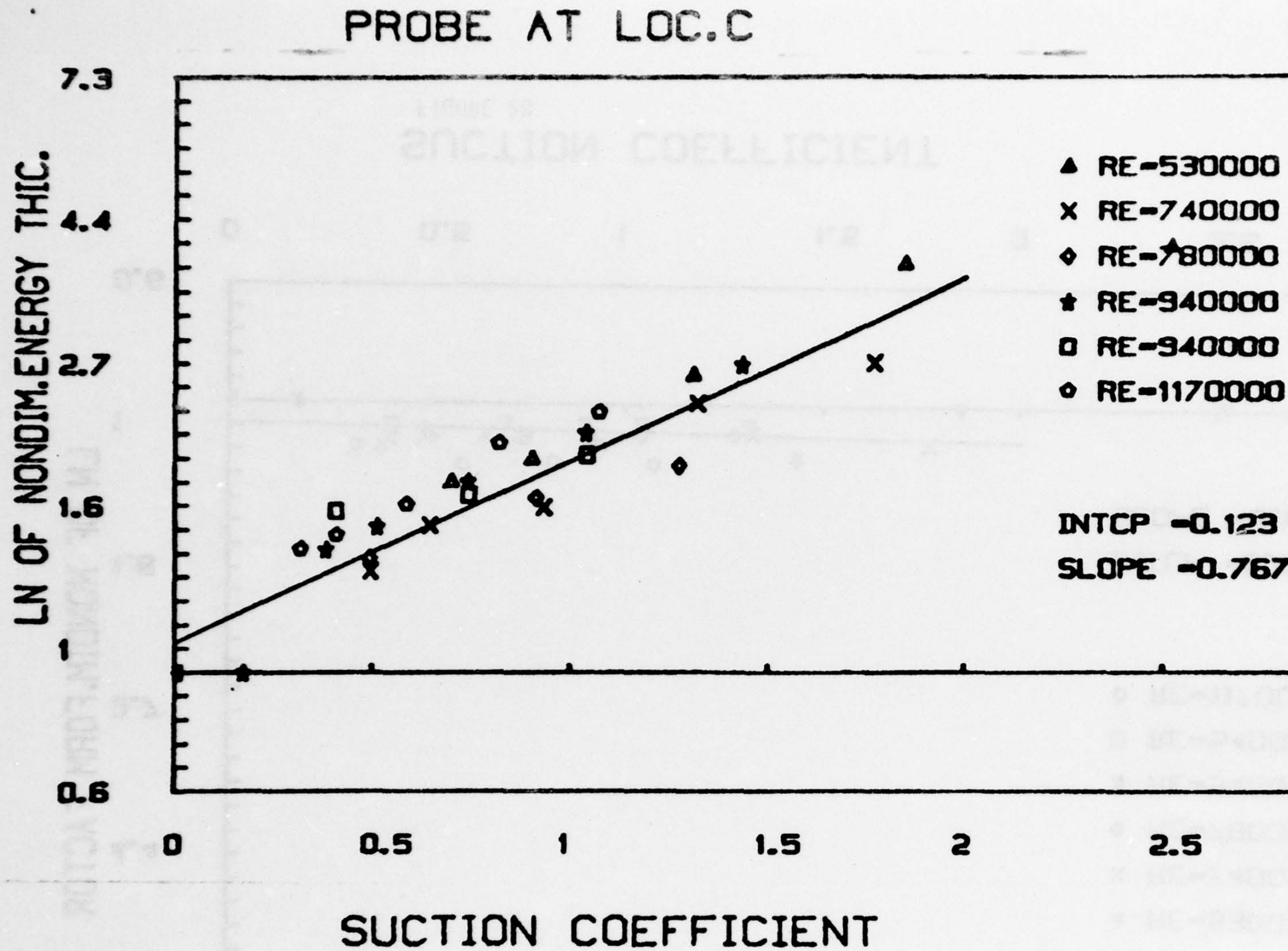
PROBE AT LOC.C
LN OF NONDIM.ENERGY THIC.
7.3
4.4
2.7
1.6
1
0.6
0
0.5
1
1.5
2
2.5
SUCTION COEFFICIENT
RE-530000
RE-740000
RE-780000
RE-940000
RE-940000
RE-1170000
INTCP -0.123
SLOPE -0.767

FIGURE 27

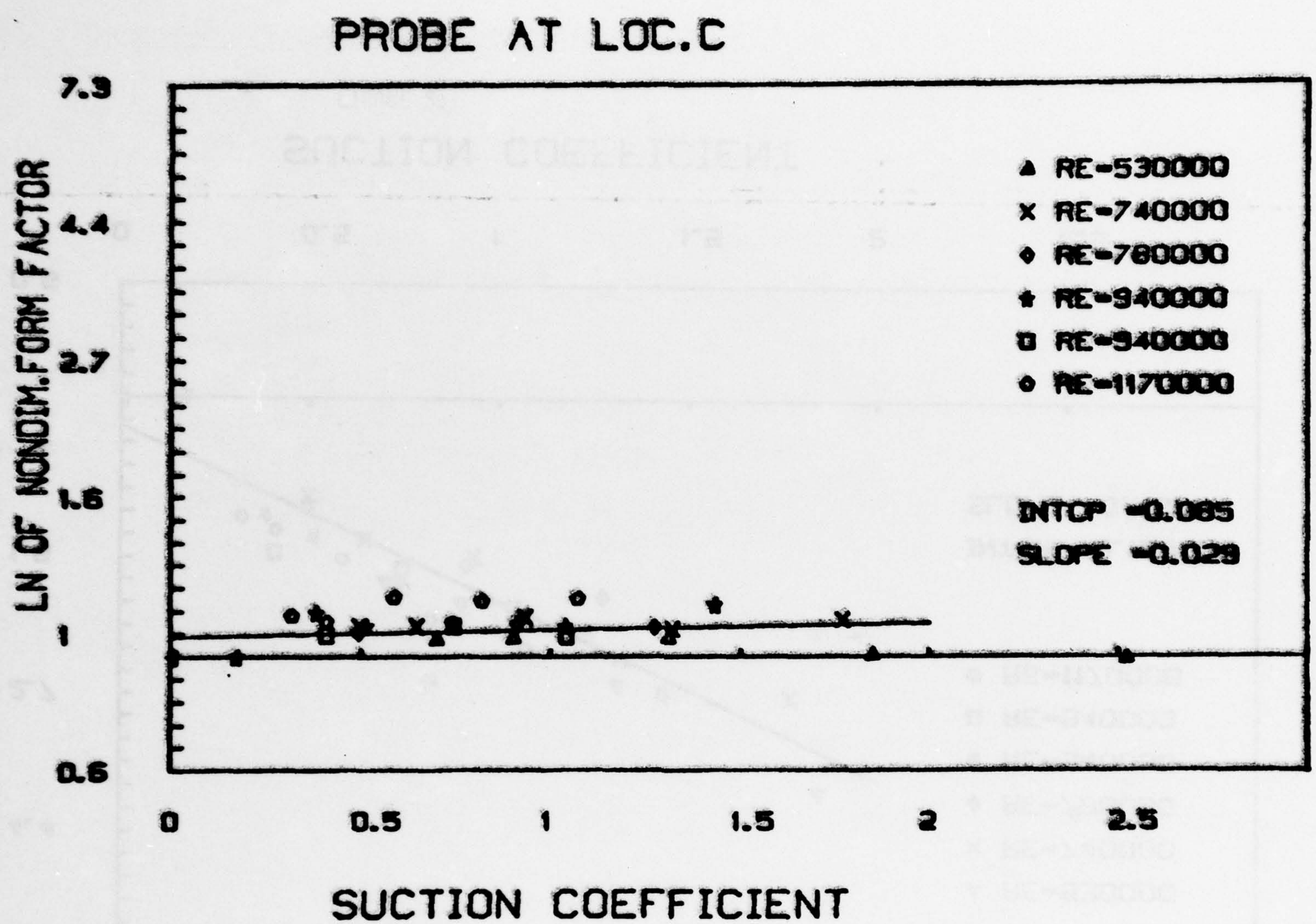
PROBE AT LOC.C
LN OF NONDIM.FORM FACTOR
7.3
4.4
2.7
1.6
1
0.6
0
0.5
1
1.5
2
2.5
SUCTION COEFFICIENT
RE=530000
RE=740000
RE=780000
RE=940000
RE=940000
RE=1170000
INTCP =0.065
SLOPE =0.029
FIGURE 28

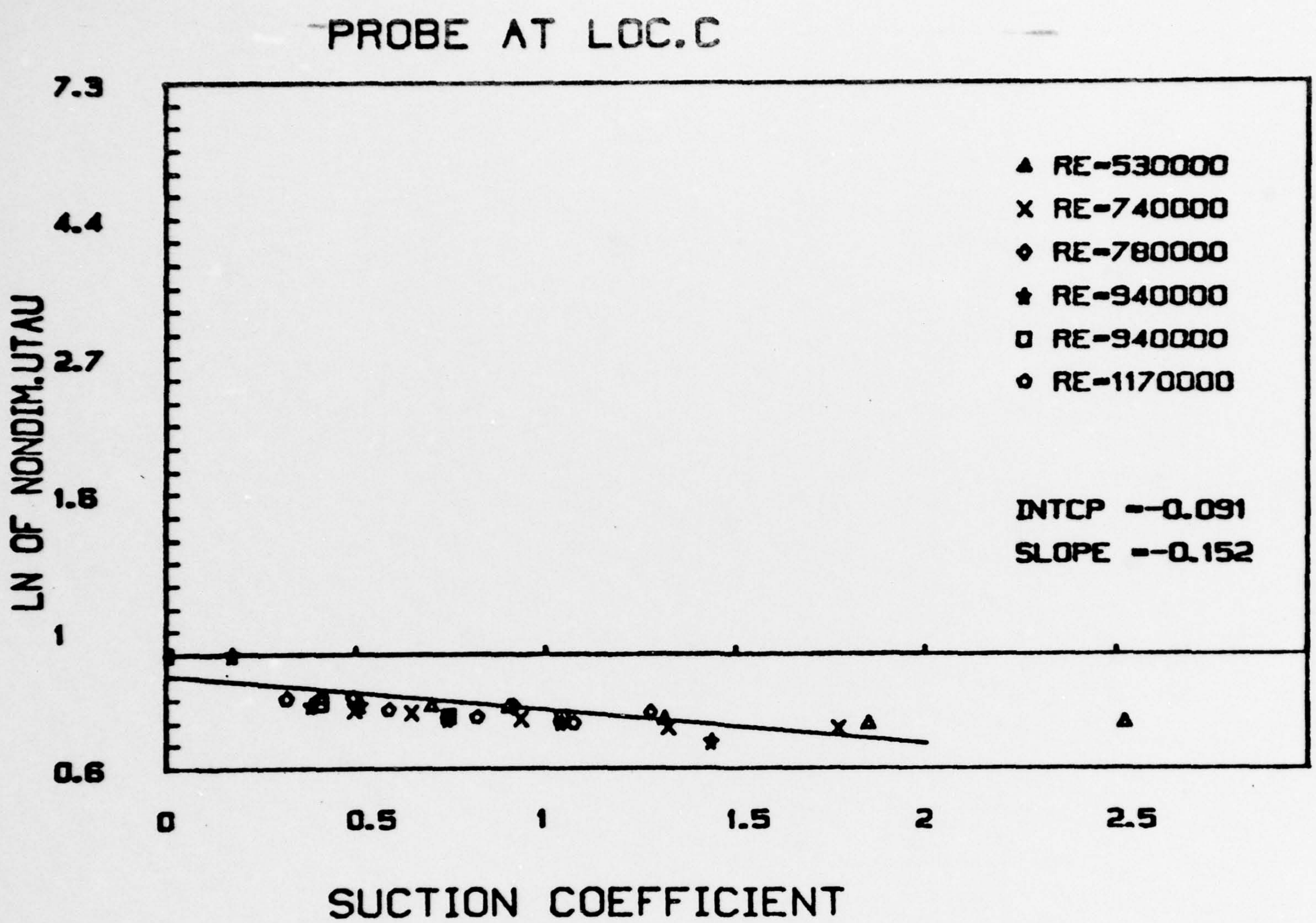
PROBE AT LOC.C
7.3
4.4
2.7
1.8
1
0.6
LN OF NONDIM.UTAU
0
0.5
1
1.5
2
2.5
SUCTION COEFFICIENT
RE=530000
RE=740000
RE=780000
RE=940000
RE=940000
RE=1170000
INTCP =-0.091
SLOPE =-0.152

FIGURE 29